Effect of Lubricant Degradation on the Tribological Performance of a Wheel-Rail System

Author: Chemical Engineer Andrey Fabio Pérez de Brito

Contact Information:

andfperezbri@unal.edu.co

Mobile: 3044372522

Universidad Nacional de Colombia

Facultad de Minas

Advisor: PhD. Alejandro Toro Betancur

OVERVIEW

In this work lubricant degradation and its relationship with tribological behavior was studied. Commercial grease (Sintono Terra HLK) and three versions of a newly developed product (Tribolub) for the Metro system of Medellín city were studied. A twin-disc testing machine was used to evaluate the effect of degradation caused by either radiation or mechanical action on the tribological properties of the greases; also, a number of tests were carried out to learn about the changes in rheological properties of the greases.

The results showed that tribological testing of degraded greases using a twin-disc machine and a subsequent viscometric analysis can be considered as a viable option to study performance of degraded greases used for wheel-rail systems. All the greases studied showed a decrease in their tribological performance after mechanical degradation in twin-disc testing machine, being the degraded Tribolub-3 the one that allowed obtaining lower values of friction coefficient and mass loss of the samples. Both mechanical and radiation-induced degradation led to a significant increase in the viscosity of the greases studied, especially for low shear rates. FTIR analyses showed that such response was mainly caused by chemical changes in the structure of the greases. Viscosity-time curves showed a rheopectic behavior at low shear rates for Sintono Terra HLK and one of the versions of Tribolub, which was related to the particle contents and the effect of thickeners. Wetting tests showed better wettability for Tribolub than for Sintono Terra HLK, both before and after degradation.

Table of Contents

Illustration Index

1 INTRODUCTION

Lubricant degradation is an important object of study for any possible applications because of different problems involved. In this case a new lubricant was developed for a massive transportation system. However there is a need to study its performance considering a plausible degradation scenario for improvement, optimizing or even changes to be made if necessary.

2 PROBLEM STATEMENT

There is no established methodology for lubricant degradation study in wheel-rail system and its performance. Therefore is necessary to establish a precedent based on previous works on this matter. This constitutes a first problem to address, being the second one to search and find proper techniques for analyzing lubricant degradation.

3 JUSTIFICATION

There are several reasons to justify this work. In the first instance, line B layout of the metro system of Medellín city with its curves and prolonged slopes showed significant wear, thus creating a need to find a suitable lubricant. However, commercial lubricants that have been tested have not proved entirely satisfactory. Then it was necessary to develop a new lubricant and in order to solve that need a new lubricant was develop by the GTS (Grupo de Tribología y Superficies) teamwork leaded by former Ph D. student Juan Felipe Santa at Universidad Nacional de Colombia. The new lubricant was called 'Tribolub'. A completely new FM to meet the requirements of the city urban train.

Given that it is a completely new lubricant and the conditions of application, this study is relevant because Tribolub's resistance to degradation is unknown and possible effects could appear on the tribological performance which in turn may result in an economic cost if the lubricant developed at this stage is not adequate or is found lacking adequate resistance to a possible degradation scenario.

Considering that 'Tribolub' is a completely new lubricant different tests are required in order to take it from prototype level and transform it into a consolidated product ready for commercial use.

4 OBJECTIVES

4.1 GENERAL OBJECTIVE

To evaluate lubricant degradation and its relationship with tribological performance in rolling-sliding conditions equivalent to those found in a wheel-rail system.

4.2 SPECIFIC OBJECTIVES

- To identify lubricant degradation mechanisms due to its application in the tribological system.
- To study some aspects of the Solid-Liquid Interaction in order to items to discuss the mechanisms of degradation of the lubricant.
- To adapting a method to make the study of lubricant degradation in the laboratory under sliding rolling.
- To analyze the information obtained from the study of lubricant and establish whether or not a significant effect of degradation on tribological performance.

5 THEORETICAL FRAMEWORK

Controlling both friction and wear has been a main concern for any developing civilization throughout history. Reducing friction to acceptable levels may increase productivity of equipments, machines or any device involved. For achieving this objective lubricants constitute an important option.

However, to understand this problem first we need to analyze what is friction and how we could classify it.

5.1 Friction

Several definitions according to experts are presented to define the concept of friction.

In terms of energy, friction is defined as the loss of mechanical energy during the beginning, development and climax of a process due to the relative movement between two material interfaces in contact.

Also, friction is often described as the mechanical force which resists movement (dynamic or kinetic friction) or hinders movement (static friction) between sliding or rolling surfaces. Here we introduce different types of friction, these types are also called external friction. Internal friction results from the

friction between lubricant molecules; this is described as viscosity another important feature when describing lubricants.

There as different causes of external friction, the main one is the microscopic contact points between two sliding surfaces; these are the cause of adhesion, material deformation, and grooving. Energy which is lost as friction can be measured as heat and/or mechanical vibration. Lubricants should be designed to reduce or avoid the micro-contact which causes external friction.

5.1.1 Sliding Friction

This is friction in a pure sliding motion without rolling and or spinning (As seen in Fig. 5.1). Figure 5.3 defines the coefficient of friction as the dimensionless ratio of the friction force F and the normal force N. The proportionality between normal force and frictional force is often given in dry and boundary friction conditions but not in fluid-film lubrication.
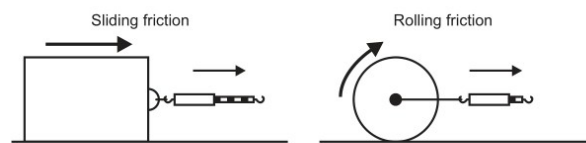
Figure 5.1: Sliding and rolling friction.
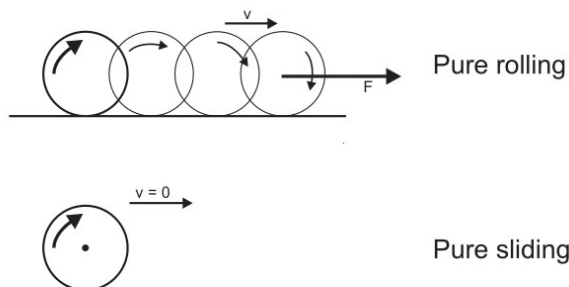
Figure 5.2: Pure rolling
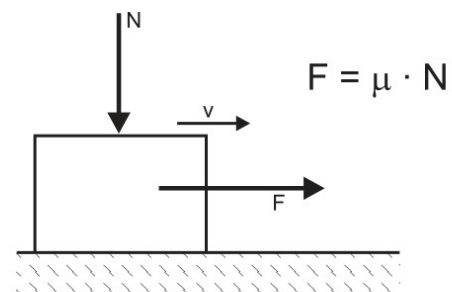
Figure 5.3: Pure sliding.

5.1.2 Rolling Friction

This type of friction is generated by rolling contact (As seen above in Fig. 5.2). In roller bearings, rolling friction mainly occurs between the rolling elements and the raceways, whereas sliding friction occurs between the rolling elements and the cage. The main cause of friction in roller bearings is sliding in the contact zones between the rolling elements and the raceways. It is also influenced by the geometry of the contacting surfaces and the deformation of the contacting elements. In addition, sliding also occurs between the cage pockets and the rolling elements. (1) A wheel-rail system could be considered analogous to the case of a roller bearing being the raceway the rail in this case and the locomotive wheels the rolling elements.

If rolling motion and sliding motion combine to any significant extent, as for gear tooth meshing, special terminology has been created. The word 'Wälzreibung' which is derived from 'Wälzen' (rolling, e.g. steel rolling) was first introduced in Germany where is primarily used. It is important to consider that situations in which a high sliding/rolling ratio occur require totally different lubrication than does pure sliding. Figure 5.2 shows this 'rolling friction' during rolling and during gear meshing.

Lubricant stability under this combination of rolling and sliding motion is an important characteristic for the proposed study object for Tribolub, the lubricant developed by GTS at Universidad Nacional.

5.1.3 Stribeck Diagram

The friction or lubrication conditions between boundary and fluid friction are graphically illustrated by use of Stribeck diagram (Fig. 5.4).These are based on the starting-up of a plain bearing whose shaft and bearing shells are, when stationary, separated only by a molecular lubricant layer. As the speed of revolution of the shaft increases (peripheral speed) a thicker hydrodynamic lubricant film is created what initially causes sporadic mixed friction but which, nevertheless, significantly reduces the coefficient of friction. As the speed continues to increase, a full, uninterrupted film is formed over the entire bearing faces; this sharply reduces the coefficient of friction. As speed increases, internal friction in the lubricating film adds to external friction. The curve passes a minimum coefficient of friction value and then increases, solely as a result of internal friction.

As shown in Fig. 5.4 lubricant film thickness depends on the friction and lubrication conditions including the surface roughness, R.

5.1.4 Hydrodynamic Lubrication

Figure 5.4 demonstrates the formation of a hydrodynamic liquid film. The lubricant is pulled into the conical converging clearance by the rotation of the shaft. The created dynamic pressure carries the shaft.

On the basis of the Navier–Stokes theory of fluid mechanics, Reynolds created the basic formula for hydrodynamic lubrication in 1886. Several criteria remained excluded, however, especially the influence of pressure and temperature on viscosity.

The application of the Reynolds' formula led to theoretical calculations on plain bearings. The only lubricant value was viscosity.
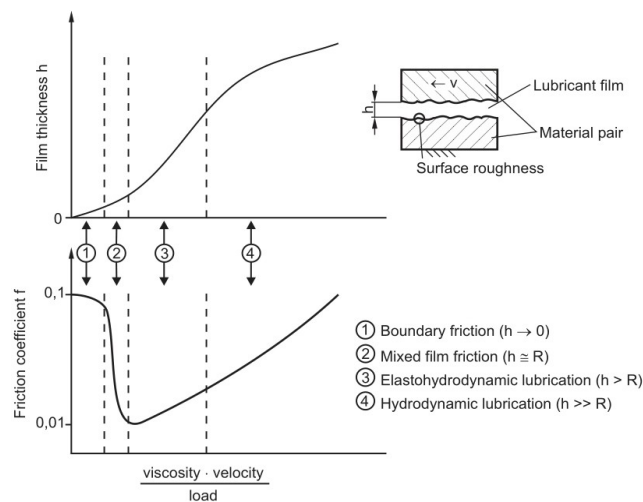
Figure 5.4: Stribeck diagram.

5.2 Lubricants

Most lubricants are made from mineral oils as a basis constituting 90% of the entire formulation, the following 10% corresponds to different additives added to achieve certain characteristics. Although mineral oils are commonly used, nowadays different vegetal and synthetic oils are also being used. (1)

Additives help to reduce friction and thus wear, increase viscosity and giving the lubricant oxidation resistance qualities, in other words the ability to endure degradation.

A lubricant is a substance introduced to reduce friction between surfaces in contact. Property which is also known as lubricity. Liquid lubricants, however, also have desirable secondary properties and characteristics:

They can be drawn between moving parts by hydraulic action.

They have relatively high heat-sink capacity to cool the contacting parts.

They are easily mixed with chemicals to give a variety of properties such as corrosion resistance, detergency, or surface-active layers.

Lubricants have the following characteristics:

- High boiling point.
- Low fusion point.
- High viscosity index.

- Thermal stability.
- Protection against corrosion.
- High oxidative resistance.

Lubricants can be divided into those of petroleum origin, known as "mineral oils," and those of animal or vegetable origin, known as "fatty oils." Synthetic oils are often grouped with the latter. In order for a lubricant to be effective, it must be viscous enough to maintain a lubricant film under operating conditions but should be as fluid as possible to remove heat and to avoid power loss due to viscous drag. (3)

A lubricant should also be stable under thermal and oxidation stresses, have low volatility, and possess some ability to control friction and wear by itself. (3)

5.2.1 Petroleum or Mineral Oil Base Stocks

Petroleum or mineral oils are generally complex mixtures of hydrocarbons but can roughly be divided according to the chemical family to which their predominating constituents belong, as paraffins or naphthenes (sometimes referred to as cycloparafins). Paraffinic oils are characterized by their pour points, usually -17.8 to -6.7 °C, and by a moderate change in viscosity with an increase in temperature. In general, their viscosity index will range from 85 to 100. Paraffinic oils have a lower density than naphthenic oils. Naphthenic oils are characterized by pour points from -50 to -12° C and a larger change in viscosity with an increase in temperature. In general, their viscosity index will range from 0 to 60. Both naphthenic and paraffinic oils have a wide range of flash and fire points.

5.2.2 Synthetic Oil Base Stocks

Synthetic lubricants have the potential of satisfying a wide range of requirements, since they can be formulated with nearly any desired range of a specific property. However, certain other properties fixed by the chemical structures must be accepted in many cases. Applications must be considered in terms of all properties associated with the proposed synthetic fluid. Choosing the right synthetic fluid can be tricky because to get special characteristics the user usually must trade off some other performance feature. Generally, synthetics have good thermal and oxidation stability, but a common weakness is limited lubricity (the ability of the lubricant to reduce wear and friction other than by its purely viscous properties). In general, synthetic oils cost considerably more per unit volume than the petroleum oils they replace. However, the real value of the lubricant must be calculated on a price-for-performance basis.

5.2.3 Grease Base Stocks

A petroleum grease is a lubricating oil to which a thickener has been added, usually a metallic soap. The type of thickener added determines the characteristics of the grease. Greases are preferred to liquid lubricants when the application of a continuous supply of lubricant is impractical. Greases are also preferred when equipment is not readily accessible and when a sufficiently tight enclosure for retaining a liquid lubricant does not exist.

5.2.4 Lubricating Oil

Lubricating oil is the largest single component of a lubricating grease and is the component that provides the grease with its ability to lubricate. Simple greases, only oil and thickener, usually contain 65 to 95% oil. Although the retentive properties of grease, as well as its resistance to heat, water, and extreme loads, depend upon the proportion and type of soap, the frictional characteristics of grease are based on its oil content. The more important oil properties affecting overall grease performance are as follows:

1. Viscosity and viscosity-temperature characteristics, which influence the ability of a grease to form a lubricating film in service and also influence its behavior at low temperatures .

2. Oxidation resistance and evaporation characteristics, which influence the ability of a grease to lubricate for extended times, especially at higher temperatures .

3. Characteristics affecting elastomers, which influence the compatibility of a grease with seal materials used in bearings and other devices Most greases employ a petroleum-based oil as the lubricating oil, but some use synthetic fluids. Diesters, silicones, polyol esters, polyalkylene glycols, and fluorosilicones are most commonly used. These fluids offer special characteristics, such as high-temperature performance, chemical resistance, and low temperature performance, that elude refined petroleum oils. Their cost is substantially higher than that of the refined petroleum oils.

5.2.5 Lubricant Additives

As was already mentioned, industrial lubricants consist of 75-90% by volume base oil, and the remainder percentage corresponds to different additives. A wide variety of additives are applied in lubricant formulation. Here there is a review of the most important ones:

Boundry and extreme pressure lubricant (lubricity) addittives. When asperity contact takes place, it is beneficial to have a protective lubricant coating to reduce friction and wear.

Biocides. Oil and additives such as emulsifiers are subject to biological attack in solution. For this reason, biocides are added to the base oil to control the activity of microorganisms and extend the useful life of lubricants. The development of biocides is the topic of ongoing research, since the environmental implications of lubricant disposal conflict with the need for biodegradation resistance during use.

Alkalinity addittives. In naval applications, it is common to use a high sulfur fuel, which results in SO_2 and SO_3 combustion products. These can cause acidic corrosion of machine elements, which is avoided through additives that increase the alkalinity of the lubricant.(3)

Detergents. Especially in diesel engines, carbon particulate can become suspended in the lubricant and can coat and foul machine elements. Detergent additives maintain a suspension of particles, prolonging lubricant life.

Antifoaming addittives. Antifoaming additives are added to ensure proper flooding of contacts and pump operation.

Demulsibility addittives. For marine applications, it is possible that lubricant can become contaminated with water. Additives that force rapid separation of the water from the lubricant are utilized for these applications.

Antioxidants. decrease the rate of oxidation of oil, which is especially important at elevated temperatures.

Viscosity addittives. Incorporated into certain industrial lubricants as described above.

5.3 Lubrication in Railway Systems

In a railway systems lubrication is centered in three main fields; locomotive lubrication, switch lubrication and wheel-rail or track-side lubrication. Being the last two applications the main concern of this work.

Depending on the design of the driving system of the locomotive a gear oil or a gear grease is required. The poor sealing properties of these kind of gears lead to leakage; this is usually minimized by use of bitumen-based products. Modern greases are thickened with lithium or sodium soap and based on mineral oils of up to 2000 mm^2 s–1 at 40ºC. Traction motor gear greases are not described in terms of consistency; the apparent viscosity is usually checked with a Brookfield viscometer, for example with a number 3 spindle at 93ºC and at 4 rpm and giving values of 5000 to 10,000 cP. (1) Although this methodology is mainly used for locomotive gear greases, it could be useful for checking viscosity of friction modifiers.

The axle bearings are greased with conventional lithium EP greases. The development of ready-to-build-in axle boxes and the increasing speed of modern trains have led to improvement of the high-temperature performance and lifetime of greases.

Switch lubrication, wheel flange lubrication (mainly used in Europe), and rail track-side lubrication in curves, used mainly in the USA and Canada, cause environmental problems. Biodegradable greases based on esters have better wear-protection and consumption performance. It is important to note that these greases must be sprayable because of the means of application.

Wheel flange and track side lubrication are also well known solutions for reducing curve squeal by using either lubricant grease or water. Both of them work by reducing the coefficient of friction, and thereby also the difference between static and sliding friction coefficients. If lubricants are used, it must be ensured that they do not lead to loss of adhesion and thus compromise safety.

Lubricant grease reduces the coefficient of friction to below 0.2 and is therefore normally only applied to the rail gauge corner or wheel flange. Although this may not be the primary cause of squeal noise, it

is possible that it reduces the occurrence of squeal by modifying the curving behaviour, i.e. reducing the angle of attack.

5.4 Friction Modifiers

Friction modifiers, which are applied to the wheel tread or top of rail to produce and maintain a specific level of friction, have emerged as effective tools for controlling friction. They do, however, require a greater degree of system control and applicator reliability. (4)

Friction modifiers act by reducing or eliminating the falling friction characteristic without reducing the level of friction too much. In some cases the friction modifier actually gives a friction characteristic that continues to rise with increasing creepage.

5.5 Lubrication systems

The first issue to analyze a lubrication system is the power required to pump the FM, which is related to the shear stress velocity flow and time requires, to pump a certain amount of the FM. An initial estimate calculated from the area under the curve for certain rheometric tests, according to which, the power to pump 200 ml per second is 240 W. However, in this estimation, the losses by pressure in the pipes and nozzle are not included.

5.6 Tribolub Development

Tribolub was developed by GTS in order to comply with the needs of the Medellín Metro. It consists of the following components:

- Molybdenum disulfide Solid Lubricant
- Graphite
- Cab-o-Sil
- Copper particles
- Silica particles
- Nickel particles
- Antioxidants
- Calcium Carbonate

After obtaining proper particle contents, the final formula was obtained by adding thickeners to the base oil an after that the solution was homogenized by mechanical stirring and an ultrasonic bath at temperature of 40ºC.

Afterwards, other particles (including thickeners) were added to the base oil and the solution was homogenized by mechanical stirring. (5)
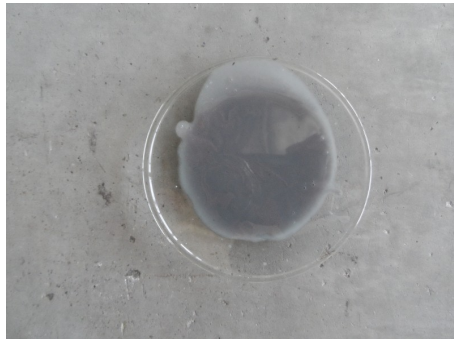
Figure 5.5: Tribolub-2
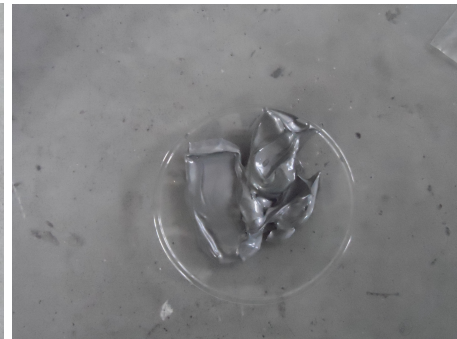
Figure 5.6: Sintono Terra HLK

5.7 Rheology of Lubricants

There are several key parameters such as consistency, flow properties, or viscosity in the case of oils, that are vital to attain lubrication efficiency in the application of lubricants. These are common terms which appear in nearly all lubricant specifications. Among these terms, viscosity is also the only lubricant value which is adopted into the design process for hydrodynamic and elastohydrodynamic lubrication.

There are different ways to study the rheology of lubricants. However the ones chosen for developing this work are comprised in what is called rotational rheology.

5.8 Viscosity

When friction is generated by a fluid surrounding contacting partners, i.e. without contact of the partners, is the internal friction of the fluid. In the right-hand branch of the Stribeck graph, internal friction increases with bearing speed. The measure of internal friction in a fluid is defined as viscosity. Viscosity and its dimensions are best explained with a model of parallel layers of fluid which could be viewed molecularly (Fig. 5.7).

If this packet of fluid layers is sheared (s), the individual fluid layers are displaced in the direction of the shearing force. The upper layers move more rapidly than the lower layers because molecular forces act to resist movement between the layers. These forces create resistance to shearing and this resistance is given the term dynamic viscosity.
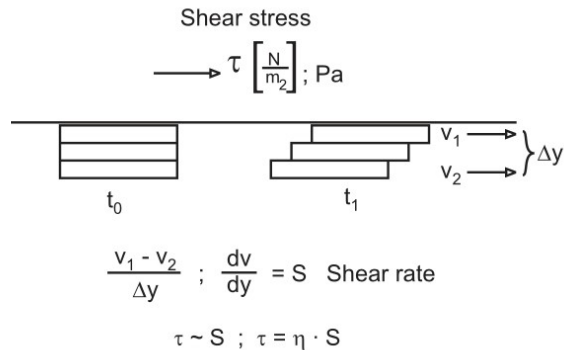
Figure 5.7: Explanation of viscosity.

Shear rate -denoted as S- consist of the difference in velocity between two given fluid layers, related to their linear displacement. This velocity gradient is proportional to the shear stress (s). The proportionality constant g is called dynamic viscosity and has the units Pa · s.
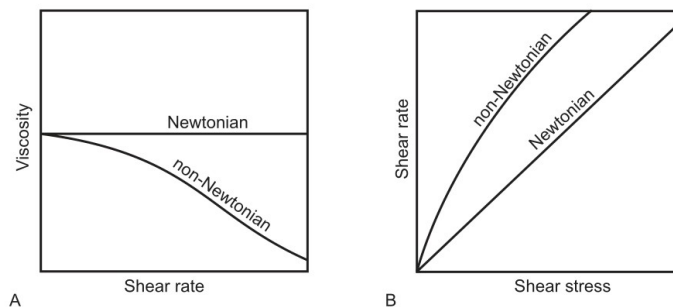
Figure 5.8: Flow characteristics of Newtonian and non-Newtonian lubricants. A. viscosity as a function of shear stress; B. shear rate as a function of shear stress.

Fluids which display the above proportionality constant between shear stress and shear rate are referred to as Newtonian fluids, i.e. the viscosity of Newtonian fluids is independent of shear rate (As seen above in Fig. 5.8). Deviations from this Newtonian behavior are sometimes referred to as structural viscosity. Those viscosities are named as apparent viscosities.

Viscosity is a vital lubricant property, influencing the ability of the oil to form a lubricating film or to minimise friction and reduce wear.

The unit of absolute viscosity is the pascal second (Pa.s), but centipoise (cP) is generally used as the alternative unit, where 1 Pa.s = 103 cP. Absolute viscosity is usually measured with rotary viscometers

19

where a rotor spins in a container of the fluid to be measured and the resistance to rotation, torque, is measured. Absolute viscosity is an important measurement for the lubricating properties of oils used in gears and bearings.

5.8.1 Influence of Temperature on Viscosity (V–T Behavior)

The viscosity of all oils used for lubrication purposes drops significantly when their temperature increases. In linear systems, this V–T behavior is hyperbolic and the practical differentiation necessary in practice is difficult to replicate and the interpolation between two measured viscosities is also problematic. For these reasons, V–T behavior has been adjusted to a function which results in a straight-line graph if suitable co-ordinates are selected.

The Ubbelohde–Walter equation has become generally accepted and also forms the basis of ASTM, ISO and DIN calculation guide lines.

$$\lg\lg (v + C) = K - m \cdot \lg T$$
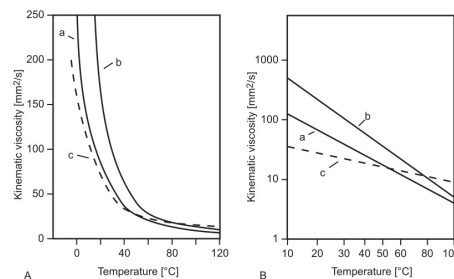
Figure 5.9: V–T behavior of various oils. A. linear; B, double-logarithmic; a, paraffinic base oil; b, naphthenic base oil; c, rapeseed oil.

5.8.2 Special Rheological Effects

Besides structure-viscosity and permanent viscosity reduction caused by shearing, lubricants are subject to further rheological effects and in particular, colloidal systems consisting of solid or fluid dispersions (solid dispersions or emulsions). In a friction modifier additives such as copper, aluminum and silica particles play an important role in these effects.

5.8.3 Shear-thinning liquids

Employing the well-defined viscometers, that could be, the small-gap, concentric-cylinder or the cone-and-plate type, we are able to measure directly the viscosity of structured liquids such as lubricants, polymer solutions, emulsions, dispersions, etc., as a function of either the applied stress or the applied shear rate. When we do this over a wide-enough range of either shear rate or shear stress, we generally see the kind of behavior shown in figure 5.11 below, when, we plot the results on logarithmic axes.
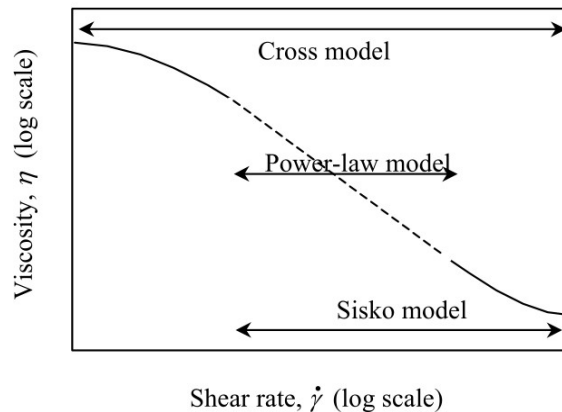
Figure 5.10: Definition diagram of the various models and the ranges that they cover.

This decrease of viscosity with shear rate is called shear thinning and must be distinguished from a decrease of viscosity with time of shearing which is called thixotropy. At some point well down the viscosity curve, we see the beginnings of a flattening out, and if data at a high-enough shear rate or shear stress is available, then a second constant viscosity region, (with value η_∞), is usually seen. Thus we have the two limiting Newtonian viscosities, η_0 and η_∞ separated by a power-law region.

5.8.4 Mathematical descriptions of flow curves

All the features of a rheogram can be captured using simple equations relating viscosity and shear rate via a minimum number of parameters.

The analysis of rheological data may be enhanced through the use of mathematical models. Non-Newtonian behavior can be simply expressed through an equation, and in some cases, the coefficients of a model can be used to infer performance of a fluid under conditions of use.

Newtonian flow is defined by a proportional response in shear stress for a change in shear rate (a linear relationship). Non-Newtonian fluids will exhibit a non- linear stress/rate relationship. Newton's equation for viscosity has been modified many times to attempt to characterize non-Newtonian behavior. Some of the more widely used equations include Bingham, Casson, NCA/CMA Casson and Power Law.

The following are some examples of just some of the simpler forms of these equations which fit different parts of the flow curve, see figure 5.12 for an overall picture. (6)
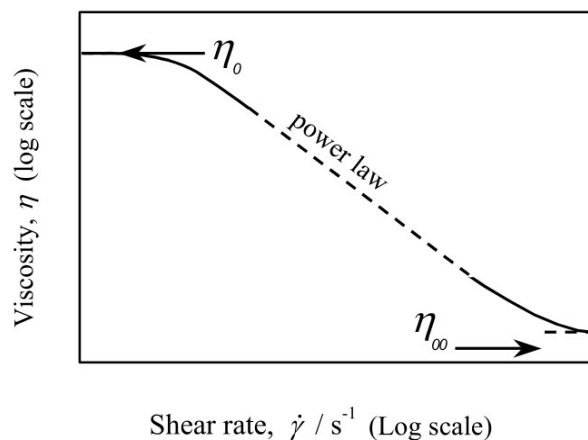
Figure 5.11: Definition diagram of parts of the flow curve.

5.8.4.1 The Cross model

First, it is important to consider one equation that describes the whole curve: this is called the Cross model, named after Malcolm Cross, an ICI rheologist who worked on dye-stuff and pigment dispersions. He found that the viscosity of many suspensions could be described by the equation of the form:

$$\frac{\eta - \eta_\infty}{\eta_o - \eta_\infty} = \frac{1}{1 + (K\dot{\gamma})^m}$$

where, written in this particular way, K has the dimensions of time, and m is dimensionless. When this model is used to describe non-Newtonian liquids, the degree of shear thinning is dictated by the value

22

of m, with m tending to zero describes more Newtonian liquids, while the most shear-thinning liquids have a value of m tending to unity.

By making various simplifying assumptions, the Cross equation can be reduced to Sisko, Power-law and Newtonian behaviour. There is another Cross-like model which uses the stress rather than the shear rate as the independent variable, it has been called the Ellis or sometimes the Meter model, and for some specific values of the exponent, it has been gives other names: for an exponent of unity it has been called the Williamson or Dougherty and Krieger model, while for an exponent of two it has been called the Philippoff model, etc.

5.8.4.2 Carreau model

The Carreau model is very similar to the Cross model, but with the whole of the bottom line within brackets. The two are the same at very low and very high shear rates, and only differ slightly at $K \dot{\gamma}$ ~ 1.

5.8.4.3 The Power-law liquid

In many situations, $\eta_0 \gg \eta_\infty$, $K \dot{\gamma} \gg 1$, and η_∞ is small. Then the Cross equation (with a simple change of the variables K and m) reduces to the well-known power-law (or Ostwald-de Waele) model, which is given by :

$$\sigma = k\dot{\gamma}^n \ or \ \eta = k\dot{\gamma}^{n-1}$$

where k is called the consistency and n the power-law index.

5.8.4.4 The Sisko model

Many real flows take place for structured liquids at shear rates where the viscosity is just coming out of the power-law region of the flow curve and flattening off towards η_∞. This situation is easily dealt with by simply adding a Newtonian contribution to the power-law description of the viscosity, giving :

$$\eta = k\dot{\gamma}^{n-1} + \eta_\infty$$, where $K^n = k$

or in terms of shear stress:

$$\sigma = k\dot{\gamma}^n + \eta_\infty\dot{\gamma}$$

This is called the Sisko equation, and it is very good at describing the flow behavior of most emulsions and suspensions in the practical everyday shear rate range of 0.1 to 1000 s-1.

5.8.4.5 Herschel-Bulkley model

The Herschel-Bulkley model is simply the Power Law model with the addition of τ_o for yield stress. Yield stress, τ_o, denotes how much shear stress is required to initiate flow. This model also provides a consistency index, k, which is a product's viscosity at 1 reciprocal second, and a flow index, n, which indicates the degree with which a material exhibits non-Newtonian flow behavior.

Since Newtonian materials have linear shear stress vs. shear rate behavior and n describes the degree of non-Newtonian flow, the flow index essentially indicates how "non-linear" a material is. For Herschel-Bulkley fluids, n will always be greater than or less than 1.

When $n < 1$ the product is shear-thinning or Pseudoplastic. This means the apparent viscosity decreases as shear rate increases. The closer n is to 0, the more shear thinning the material is.

When $n > 1$ the product is shear-thickening or Dilatant. It's apparent viscosity increases as shear rate increases.

5.9 Wetting

Wetting usually occurs within an environment that may consist of a gas or another immiscible liquid, each of which may be referred to as a fluid. A wetting system is characterized by a contact angle (CA), which is defined as the angle between the tangent to the liquid–fluid interface and the tangent to the solid surface at the contact line between the three phases (Fig. 5.12). (7)
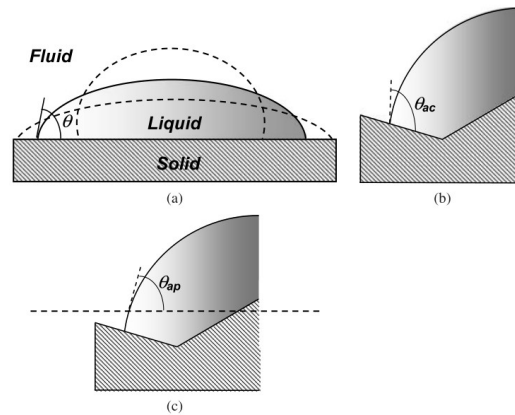
Figure 5.12: Wetting system.

Wetting is the ability of a liquid to maintain contact with a solid surface, resulting from intermolecular interactions when the two are brought together. The degree of wetting (wettability) is determined by a force balance between adhesive and cohesive forces. (8)

On a wheel-rail system the phases present are, solid; rail and liquid; friction modifier.

5.10 Degradation process

The service life of a lubricant, is basically the period of time it will function either in the machine or in this case on the surface of the rail until the antioxidants are consumed in the process which are produced significant changes in the physical and chemical properties due to oxidation. The lubricant service life is directly related to the oxidation stability thereof, and consequently to the still possessing antioxidant capacity. This antioxidant capacity is clearly related to the degree of damage that has already suffered the lubricant, so determine and identify the oxidation products presented also enables us to estimate their service life.

The root causes most affecting the service life of a lubricant air intake to the system, high temperature, oil compatibility with the material from which is made the system, condensation or water entering the system, pollution, loss of corrosion inhibitors, etc..

5.10.1   Oxidation of Hydrocarbons at Low Temperature (30–120◦ C)

The self-accelerating oxidation of hydrocarbons is called autoxidation. Its initial stage is characterised by a slow reaction with oxygen followed by a phase of increased conversion until the process comes

to a standstill. The degradation is driven by an autocatalytic reaction described by the well-established free radical mechanism, consisting of four distinct stages:

- Initiation of the radical chain reaction,
- Chain branching,
- Propagation of the radical chain reaction,
- Termination of the radical chain reaction.

5.10.2   Oxidation of Hydrocarbons at High Temperature (>120∘ C)

During oxidative and thermal degradation at high temperatures, hydrocarbons are subject to thermal cracking, namely the breakdown of their chains and as a result, compounds are formed due to chemical changes undergone by the organic compound. The problem of lubricant deterioration due to premature degradation could be caused by deterioration of oxidation inhibitors and the reaction of the metals present with the decomposition products from various additives added to obtain different characteristics. (9)

Above 120 ºC the degradation process can be divided into a primary and a secondary oxidation phase.

Primary oxidation phase: Initiation and propagation of the radical chain reaction are the same as discussed under low-temperature conditions, but selectivity is reduced and reaction rates increased. At high temperature the cleavage of hydroperoxides plays the most important role.

In order to study the degradation phenomena of a lubricant is helpful to understand the degradation products. Basically, these groups can be included in certain products which are compounds such as oxygen radicals ROO, RO, OH, R-CO-OO, etc.. (9)

The time it takes to begin an oil to oxidize under given conditions depends on the nature of the base oil as the type and concentration of the antioxidants. There are several stages in the degradation of an oil:

- Loss of antioxidants. Consider the initial stage of degradation.
- Appearance of metal salts, sulfoxides and peroxides, products from additives and oil oxidation mark a second stage of the process.
- Hydroperoxide formation which induce oxidation side reactions. Metal salts are generally identified, metal sulfates and carboxylic acids. This could be consider as a last step in lubricant degradation.

The breakdown of the lubricant can be produced by some of the following mechanisms:
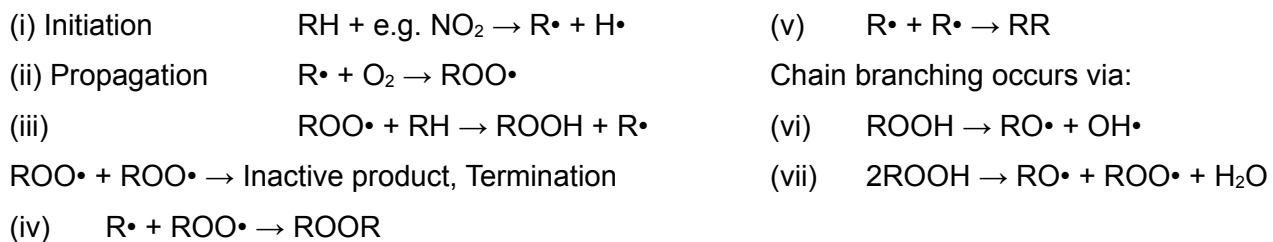
Oxidation. The double bonds are attacked by oxygen. Form acid, alcohols and aldehydes.

Hydrolysis. The water making them attacks fatty acids and alcohols. The pH decreases.

Thermal degradation. Polymerization due to high pressure and temperature form new products

Evaporation. Volatile compounds disappear due to the high temperature.

Oxidation of base oil in a free radical process in solution can be represented by the following series of reactions, Reaction sequence (i–vii): (10)

(i) Initiation $\quad\quad\quad$ RH + e.g. $NO_2 \rightarrow R\bullet + H\bullet$ $\quad\quad$ (v) $\quad$ $R\bullet + R\bullet \rightarrow RR$

(ii) Propagation $\quad\quad$ $R\bullet + O_2 \rightarrow ROO\bullet$ $\quad\quad\quad\quad\quad$ Chain branching occurs via:

(iii) $\quad\quad\quad\quad\quad$ $ROO\bullet + RH \rightarrow ROOH + R\bullet$ $\quad$ (vi) $\quad$ $ROOH \rightarrow RO\bullet + OH\bullet$

$ROO\bullet + ROO\bullet \rightarrow$ Inactive product, Termination $\quad$ (vii) $\quad$ $2ROOH \rightarrow RO\bullet + ROO\bullet + H_2O$

(iv) $\quad$ $R\bullet + ROO\bullet \rightarrow ROOR$

5.10.3 $\quad$ Inhibition of Oxidative Degradation of Lubricants

The use of additives to control lubricant degradation requires a focus on alkyl radicals (R), alkylperoxy radicals (ROO) and hydroperoxides (ROOH). Primary alkoxy radicals (RCH_2O) and hydroxy radicals (HO) rapidly abstract hydrogen from the substrate. It is therefore very unlikely that they can be deactivated by natural or synthetic antioxidants. In practice, three additive types have proven to be successful in controlling the degradation of lubricating oils:

- Radical Scavengers.
- Hydroperoxide Decomposers.
- Synergistic Mixtures Of These.

Inhibition of oxidation occurs by the prevention of chain propagation, Equation (ii) or (iii). Hindered phenols and aromatic amines donate a hydrogen atom to the peroxy radical, ROO. , Reaction (viii), in successful competition with Reaction (iii):

$ROO\bullet + AH + RH \rightarrow ROOH + A\bullet + RH$ $\quad\quad\quad\quad\quad$ (Reaction viii)

A• , the antioxidant radical is stabilised by resonance and is hence incapable of abstraction of a hydrogen atom from RH as required in Reaction (iii) and the chain reaction is thereby broken. Frequently A• radical will react with another radical, ROO• or A• , to give a stable end product.

As long as an oil is protected by antioxidants , oil oxidative degradation and changes in the properties of the lubricant will be minimal. Once the antioxidant is exhausted different physical changes occur in

the properties of the lubricant. Spending an oil antioxidants may eventually permit the rapid deterioration of the base oil , producing corrosive acids , varnishes and even , at final insoluble gums. (10)

Depending on the formulation of the additives and the base oil an oil degrades differently. The condensation reactions are of the "aldol condensation" resulting primary polymeric materials, which are soluble in oil, and can produce, by reaction, other polymers insoluble in the oil side, products which are muddy sediments or deposits.

Such polymers can act as "decomposer" chains in the oxidation step aged oil. As a consequence, and as the last stage of oil oxidation and the amount of carboxylic acids formed hydroperoxides may drastically reduce the secondary polymers formed.

5.10.4 Techniques for determining the oxidation state of an oil

5.10.4.1 Thermal oxidation techniques

RBOT (ASTM D-2272). This method uses a pressure container with oxygen to evaluate the oxidation stability of turbine oils New and used having the same composition (base oil and additives) in presence of water and catalytic copper 150 ºC. This test has been used for years to determine the remaining life of the oils in service. Typical times this assay are 2 to 30 hours, although there have been times up to 45 hours. A part of the problem of excessive time for analysis can also occur pressure drops during the test.

Figure 5.13: RBOT ASTM D-2272 testing device.

TOST (ASTM D-943). This method is used to evaluate the stability oxidation steam turbine oils in the presence of oxygen, water, and copper metal and steel at high temperature. This method is widely

used for estimating the oxidation stability of lubricants, especially those that are prone to water contamination. Test ends once the TAN value reached 2 mg KOH / mg sample. A test for a turbine is usually greater than 1500 hours. As a result of this dependence, the test is considered inadequate for monitoring the oil in service, even today still still used as a specific test oil. Another drawback is volatilization of low molecular weight fractions due to the test temperature.

Figure 5.14: TOST ASTM D-943 testing device.

5.10.4.2   *Calorimetric techniques*

HP-SCDSC. Is a differential thermal analytical method in which the time / temperature of the test is directly proportional to the differential heat flow between sample and reference material, wherein the integrated area under the curve measured is directly proportional to the total differential heat. This technique has recently been applied to measure the oxidation stability of various oil formulations, including turbine oil.

During the oxidation process the antioxidants are depleted. After this there is an increase of hydroperoxides. Above 120 °C these become unstable, decompose generating oxygen radical centers can take protons from hydrocarbons. This process is strongly exothermic. Therefore thermogravimetric analysis is useful for the characterization of the oxidation of lubricants. The advantages of this technique are that it is accurate only uses mg sample much faster than other techniques such RBOT and TOST and furthermore is not subject to interpretation by the operator.

5.10.4.3   *Optical techniques.*

FTIR. A complementary technique to the ones mentioned above and that has been in use for 40 years.

Nowadays is one of the most widely used techniques. Performing a wavelength scan of the sample between 400 and 4000 cm-1.

The amount of radiation transmitted for each wavelength is then used to identify the type and concentration of each component present in the lubricant. Programs are used in oil condition monitoring, providing information about the oxidation stability of lubricants.

It is noteworthy to mention that standard ASTM E2412 addresses infrared analysis of used lubricating fluids.

Petroleum, polyol ester and phosphate ester fluids have different spectra. In addition, petroleum oils are broken down into detergent (crankcase) and non-detergent (bearing and gear) oils, which exhibit different responses to IR analysis. Due to the similarity that exists between friction modifiers to this common oils is possible to expect a similar behavior using IR analysis. In the specific case of Tribolub and Sintono Terra HLK both consist of ester base oil. The IR spectra of the most common machinery lubricants are shown in Fig. 5.16.
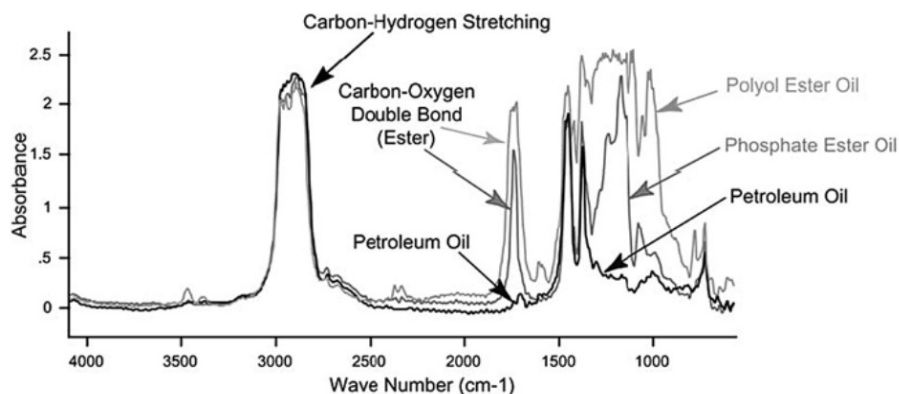

Figure 5.15: Infrared spectra for common oil types.

IR analysis help us to determine the level of oxidation by products in petroleum lubricants by means of a general response in the carbonyl region (see Fig. 5.17 below). The infrared area is measured over the range of 1800–1670 cm–1. The left baseline, high wave number side, is taken as the minimum over the region of 2200–2000 cm–1 and a right baseline, low wave number side, over the region of 600–550 cm–1. This baseline definition corrects for any offset and tilt due to soot and particulates present. (10)
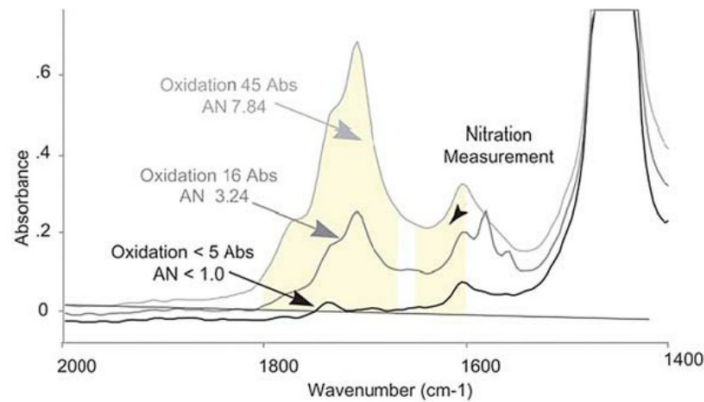
Figure 5.16: Areas of interest for oxidation by-products in petroleum oil.

Few compounds found in new and used petroleum lubricants have significant absorbance in these baseline areas. However, some additives that have minor absorbencies in this region will contribute to the overall intensity .

COLORIMETRY. Of the two techniques used in chemical oxidation based on the colorimetric method determines the hydroperoxides is faster, safer and cheaper than the method used to determine free radicals. Given the importance that should be attached to the ease and speed of analysis, we will detail the analysis for the determination of hydroperoxides. This analysis has been made and correlated with DSC technique for aviation turbine oils.

Chemiluminescence. This technique is based on the determination by phosphorescence ketones formation excited depending on the recombination of hydroperoxides. Energy emission from the sample is measured as a function of oxidation time. Is a non-destructive technique for continuous monitoring of the oxidation. Provides information on the oxidation stability of the oil and the effect of catalysis, or inhibitors. It also provides basic information on the oxidation kinetics and reaction mechanisms. The problem is that the equipment is expensive and has a very poor reproducibility. Furthermore, the sample preparation is very time consuming, as the prior chemical oxidation by colorimetry.

5.10.5   Oxidation in the wheel-rail system.

In the wheel-rail system we have the elements described above that promote lubricant oxidation. For instance we have the presence of high temperatures, up to 200ºC when a significant sliding of the wheel contact with the rail occurs (11). In addition we have air and water from coming into the system

from meteorological phenomena because is a completely open system. It is also necessary to consider the effects of UV radiation from the sun, which in this case may affect the lubricant pumped onto the tracks, since it is a transport system completely uncovered unlike and underground one. Finally, in the wheel-rail system we have the presence of metal particles, most of them ferrous in this case, which may act catalyzing the oxidation reaction of the lubricant.

It is this last feature that this work aims to study and which will be analyzed for the lubricant developed by the Tribology and Surfaces Group of the National University for use in the B line of Metro de Medellín (a prototype lubricant named 'Tribolub'), which was developed to meet the specific needs of this mass transportation system.

Since oils used as a basis for lubricant could suffer an eventual oxidation caused by high temperatures and enviromental effects, with subproducts of this reaction that could be acids and other compounds that are corrosive, degradation may hinder tribological perfomance, thus is reasonably to expect that lubricant degradation may affect the perfomance of the newly developed Tribolub.

Therefore when designing a lubricant a high oxidative resistance should be in mind. This is obtained refining the base oil and adding an inhibitor. Some of the used oxidation inhibitors are phenolic and amminic compounds. (12)

5.10.6 Problems associated with lubricant degradation.

If a lubricant exceeds its service life limit, it may cause excessive degradation of the base oil, resulting in component wear and eventual malfunction of the machine. (13) In the case of a railway and the wheel-rail system, excessive wear on the track or even on the wheels could appear and even cause safety concerns.

Controlling oxidative degradation properties of a lubricant is critical to maintaining proper operation of the machine or in the case of friction modifiers the components of railway. This is particularly important when high pressure and temperatures are involved, because these increase the cost of the lubricant antioxidants, rendering it unusable. (13)

6 BACKGROUND

Current tribological studies regarding lubricants have focused on mechanical degradation of the film on the rail. Specifically to learn regarding long the film on the surface in question before they require

reapplication of lubricant. This is known as lubricant half-life. Using for this purpose Twin-disc testing machines. (14)

Just in few cases different lubricants have been studied to determine their chemical stability against the effects of oxidation for specific use in wheel-rail system. Various additives were tested for obtaining antioxidant characteristics and finally analyzing the tribological performance as oxidation suffered by the lubricant in question. Just a few cases have studied various oils to determine their chemical stability against the effects of oxidation for specific use in wheel-rail system. (15)

In these cases tools such as FTIR spectroscopy were used along with rheological studies to analyze changes in the viscosity of the lubricant. (15)

It should be noted that the oil degradation is not new object of study but has been focused mostly on studying oils in closed systems, such as automotive engines. (6)

Therefore, it is necessary to establish a relationship between lubricant oxidation and its average life on the surface of the rail. For this it is possible to use various techniques to complete the study of lubricant degradation and help us set as will their performance in the wheel-rail system.

Additional techniques already used to study the degradation of lubricants in other systems can be; gas chromatography, liquid chromatography HPLC, TGA-DSC, and mass spectroscopy.

Another technique already used previously and successfully in the analysis of oil degradation in diverse machinery is UV-vis spectroscopy, around this technique a new generation of sensors has been developed for performing oil analysis in real time conducting an assessment of the quality of the lubricating oil and providing integrated management process for the user. These device are being implemented in order to overcome the limitations of the existing methodology of laboratory analysis it does not provide sufficiently early detection of degradation and pollution (7). In this context this work will lay the foundation for the subsequent implementation of early warning systems for the Metro de Medellín, and show the relevance of the effects of degradation on the system.

Further assays can be used to verify the wetting contact angle of the lubricant and thus determine what the adhesive performance of the lubricant film to the surface of the rail in question. In this respect wettability studies applied to the wheel-rail system have focused mostly on analyzing the changes inside the lubricant in contact angle particle effect outside it, ie different pollutants from different sources of either environmental or other oils of the carriages (18).

7 METHODOLOGY

7.1 Lubricants Characterization

The greases chosen to work with were the following; Tribolub-1 developed at Universidad Nacional de Colombia Sede Medellín, Tribolub-2 and later Tribolub-3, which constitutes an enhanced formula based on rehological studies performed on Tribolub-1 and a commercial product named Sintono Terra HLK used in the lubrication system currently installed at line B of the metro system of Medellín city.

Rheological properties were studied using two different approaches; first by means of a simple Brookfield viscometer, which is widely used in different industrial areas and then by using a more complex advanced rheometer.

7.1.1 Viscosity Tests

A conventional Brookfield LVDV-II+Pro viscometer with a temperature bath and a Bi-directional RS-232 PC Interface was used to analyze Tribolub-1, Tribolub-2, Tribolub-3 and Sintono Terra HLK at different scenarios that could describe a fluid as newtonian, non-newtonian, plastic, pseudoplastic among others. Gathering data on the lubricant's viscosity behavior gives both manufacturers and users -Metro de Medellín in this case- important knowledge of rheological characteristics valuable in predicting its pourability, its performance in a dipping or coating operation, or the ease with which it may be handled, processed, or used.

The following spindles were used for different specific tests; LV1, LV2, LV3, LV4 -these ones to get Viscosity vs speed readings -and SC4-16 with a Coaxial – cilynder measurement system- for calculating shear stress- with a maximum shear rate of 48 s-1 at 200 RPM.

For temperature control and for tests from 15ºC to 100ºC a TC-650 thermal bath was used.

Rheocalc 32 software was used to handle the information given by the viscometer.

Figure 7.1: Brookfield viscometer DV-II+Pro.

Figure 7.2: Sintono Terra HLK and SC4-16 spindle as seen inside the sample container.

7.1.1.1 Shear stress-shear rate/ Viscosity-shear rate curves

This method is also known as "Controlled Rate Ramp".

SC4-16 spindle was used to get the following flow analysis curves; Shear rate-shear stress and Viscosity-shear rate additional Viscosity- speed (RPM) curves were obtained with LV spindles that do not calculate shear rate and stress values and thus are considered as a way to obtain relative viscosity values sometimes named Brookfield viscosity.

LV1, a spindle designed for low-viscosity fluids was used to analyze Tribolub's base oil.

LV4 spindle was used to obtain Viscosity - speed (RPM) curves for Tribolub-1, -2, -3 and Sintono Terra HLK due to their higher viscosity.

This method shows how viscosity can change as a function of rotational speed or shear rate.

7.1.1.2 Viscosity - temperature curves

Viscosity of the greases was measured at different temperatures starting at 15ºC and increasing 5ºC until a maximum temperature of 75ºC was reached. Speed was set at 0.5RPM (Shear rate 0.61 s-1) for Sintono Terra HLK and 10RPM (Shear rate 12.23 s-1) for Tribolub-1, -2 and -3.

7.1.1.3 Viscosity - time curves

The greases were tested at specific shear rate which was fixed during 600 seconds in order to observe any possible changes in viscosity as time increases. Viscosity-time curves allowed to determine a possible thixotropic or rheopectic behavior for each lubricant.

7.1.1.4 Up - down shear rate curves

Basically is the same method defined above as "Controlled Rate Ramp" that is used to create the "Up Ramp". Upon reaching the maximum rotational speed or shear rate, reverse direction and return to the starting speed or shear rate, thus creatiing a "Down Ramp".

Different viscosity values indicate that the material is "time sensitive" to shearing action.

7.1.2 Rheometric tests

A Rheometer was used to study the rheological behavior and properties of the greases. Rheology tests were focused on determining particular characteristics before and after degradation, which could influence tribological behavior at the wheel-rail interface. Since the interrelation between rheology and other product dimensions often makes the measurement of viscosity the most sensitive or convenient way of detecting changes in color, density, stability, solids content, and molecular weight these tests were chosen for studying lubricant degradation.

Rheological behavior of Tribolub-1, Tribolub-2, Tribolub-3 and Sintono Terra HLK was studied at Centro de Investigación de Minerales CIMEX from Universidad Nacional de Colombia, using a Bohlin instruments C-VOR rheometer shown in Figure 7.3. The shear rate was controlled within a range from 0.1 up to 100 s-1, in addition both shear stress and viscosity were measured. A parallel plates and a cone-plate geometry was used to perform the measurements and then a model was fitted to the curves obtained.

Figure 7.3: Bohlin Instruments C-VOR rheometer.
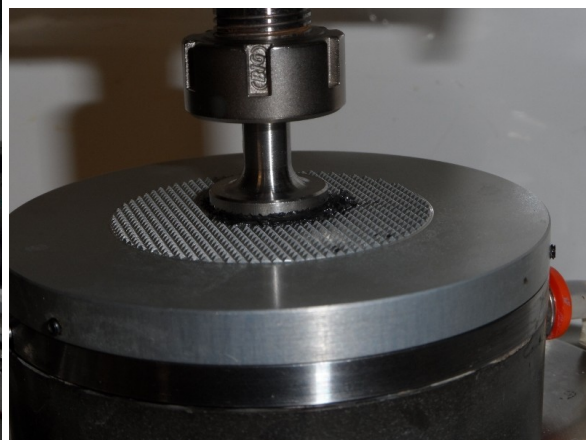
Figure 7.4: Serrated plates geometry.

7.1.3 Wettability measurements

A rail section of 5 x 8 x 14 cm was used a the selected surface before the wetting test.

A Mitutoyo SJ-201 surface roughness tester was used to check the roughness of the specific area of rail sample -the head in this case- used for wettability measurements. Figure 7.5 shows the roughness tester used and its calibration procedure.

Figure 7.5: Mitutoyo SJ-201 surface roughness tester,

Contact Angle was measured using a Dataphysics OCA Number 15 series device technique equipment.

Figure 7.6: Pendant Drop-method

Due to the extremely high viscosity of the lubricants, several mixtures were prepared, according to what is seen on the field where a mixing occurs as Locolub -a lubricant used for the train- comes in contact with the friction modifier HLK or Tribolub. Mixtures analyzed were 50 %w/w of Locolub and the respective friction modifier.

Figure 7.7: Dataphysics OCA 15. The rail sample is visible in the middle.

A syringe with a capacity of 1 mL was used to apply a drop on the selected surface - the head from a rail sample in this case-. Discrete amounts of 20 µL were dispensed to obtain a proper drop of each lubricant.

Figure 7.8: Syringe prepared for dispensing lubricant over the rail sample.
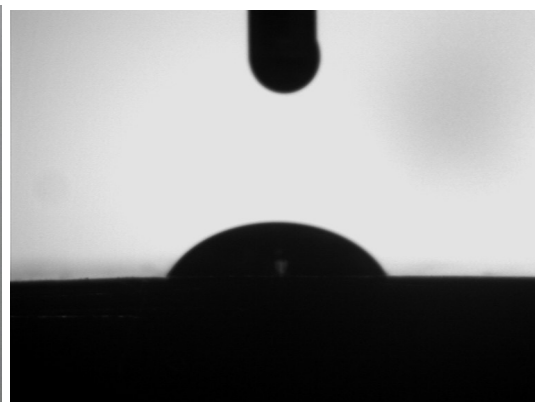
Figure 7.9: A drop of Tribolub-1 as seen through Dataphysics OCA 15 device.

7.1.4 FTIR

Samples of the greases before and after degradation were taken and analyzed with FTIR technique in order to identify changes in the structure and chemical bonding of each lubricant for different conditions of degradation, both tribological and luminic.

A Nicolet™ 6700 FT-IR device was used for obtaining each sample spectrum by performing 64 scan

sweeps with a resolution of 4 cm-1. Data analysis was performed with an OMNIC software.

7.2 Degradation tests

7.2.1 Tribological tests

For the twin discs tests, **c**ylindrical samples were manufactured from rails and wheel using a lathe. The wheel samples were extracted from ER8 wheels and according to EN 13262 standard. Rail samples samples were extracted from the head of a 370Cr HT rail.

The wheel samples were homogenized at 870ºC for 30 minutes and then air cooled. The homogenized samples were austenized at 840ºC for 30 min and then placed in a salt bath (isothermal heat treatment) at 520ºC during 30 seconds after that, the cylinders were cooled down in oil to room temperature. After heat treatment, the discs were manufactured according to the dimensions of samples for the twin-disc machine as shown in Figure 7.11.

The hardness of the wheels varied between 280 and 320 HV in all cases. On the other hand the hardness of the rails varied between 39 to 41 Hrc, 390 and 410 HV in all cases.

Twin disc tests were performed to measure the friction coefficient of the developed FM and the results were compared with those from the selected commercial product -Sintono Terra HLK-. Figure shows a general view of the device. The equipment used was a Twin-disc tribometer from Universidad Nacional de Colombia Sede Medellín.

In order to obtain degraded lubricant sample, several tests were performed at 10,000 and 20,000 cycles.

Then testing for studying tribological performance of the degraded lubricants was done at 14,000 cycle and 5% sliding conditions.

Figure 7.10: Twin-disc machine.
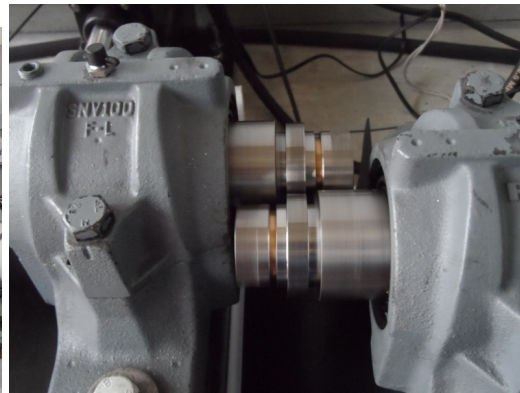
Figure 7.11: Twin-disc tribometer in motion.

For each grease, the same quantity (0.02 to 0.03 g) was applied onto the surface using a brush at intervals of 60 seconds as shown in the figure 7.12. The degraded lubricant remains were collected after each test for analysis.

Figure 7.12: Brush method used to apply a proper film of lubricant to the sample's surface.

7.2.2 Photodegradation

Photodegradation Test

Environmental degradation accounts for a significant degradation of any polymeric structure in this case a grease being the solar radiation the most damaging source. Photodegradation tests were made using the Atlas SUNTEST XLS+ device, which is a xenon tester with UV-control that performs photodegradability testing according to the ASTM D6695 and allows simulating solar radiation exposure. Tribolub-1, Tribolub-2 and HLK samples were photo degraded during; 8, 16, 24, 32, 40 and

48 hours under the following conditions:

E= 765 W/m^2

BST 40ªC (set point), 49°C (actual temperature)

CHT 35°C (sensor).

Figure 7.13: Atlas Sun Test XLS+ device.

Figure 7.14: Photodegraded sample of Tribolub-1.

After the photodegradation some samples were selected as follows; for Sintono Terra HLK, Tribolub-3 and its previous generations samples photodegraded for 48 hours.

7.3 Particle analysis

7.3.1.1 Optical Microscope

A Nikon PME3 Light Optical Microscope was used to analyze particle distribution and morphology. Samples were obtained by using a brush to apply a thin coating of each lubricant onto a glass slide.

Sintono Terra HLK and Tribolub-3 with its respective degraded counterparts were analyzed.

Images were taken at the following magnifications; 5X,10X,20X,50X and 100X.
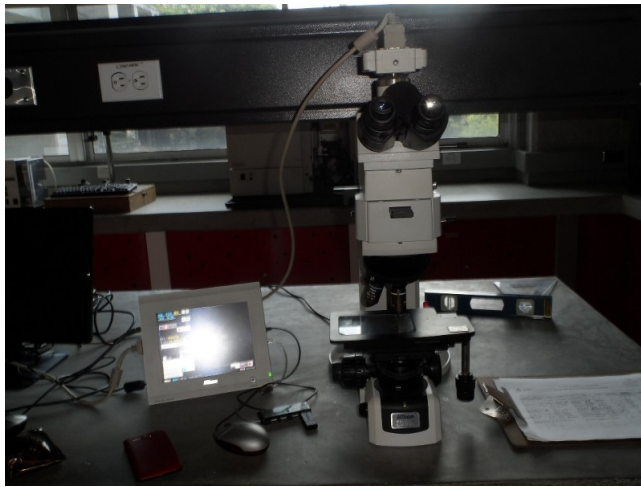
Figure 7.15: Optical microscope.
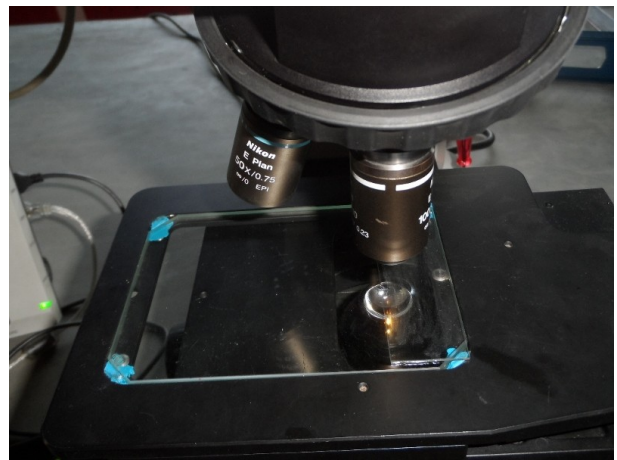
Figure 7.16: Lubricant sample on a glass slide.

7.3.1.2 SEM

Scanning electron microscope technique was used for analyzing particle morphology of Sintono Terra HLK and Tribolub-3 before and after suffering degradation. Particles present in the lubricants were studied using a JEOL 5910LV Scanning Electron Microscope (SEM).

Micro analysis of the lubricant samples were carried out in an Energy Dispersive X-Ray Spectrometer (EDXS) coupled to the SEM device.

8 RESULTS

8.1 Viscometric Tests

8.1.1 Viscosity vs Temperature curves

Viscosity-temperature curves for Tribolub-2 and Tribolub-3 are shown in figures 8.1 and 8.2
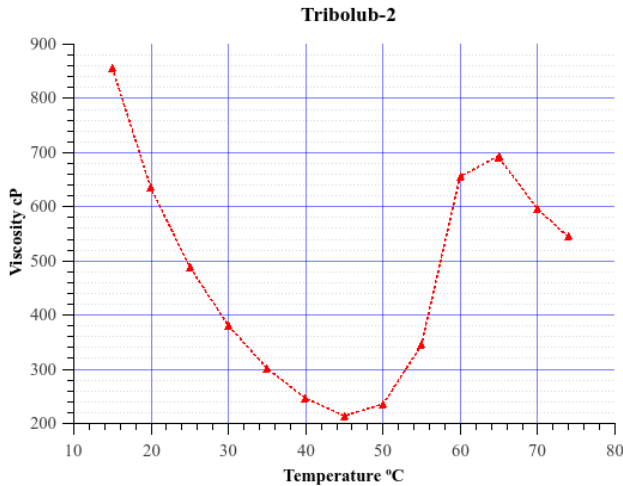
Figure 8.1: Tribolub-2 temperature curve.
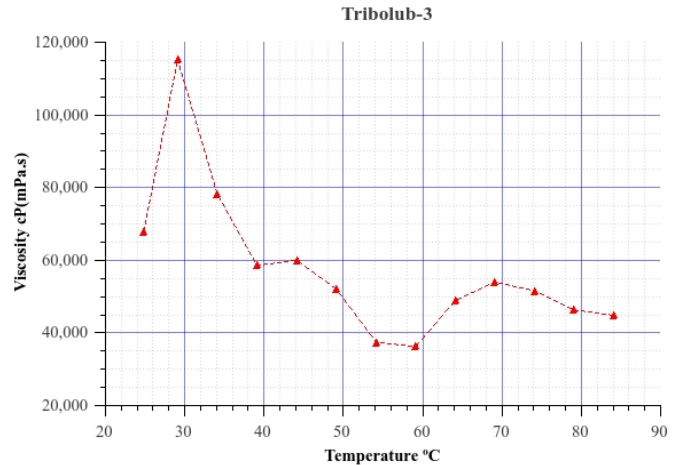
Figure 8.2: Tribolub-3 temperature curve.

Tribolub-2 shows a particular behavior. Rather than a linear decrease in viscosity, it suffers and increase at 45ºC climaxing at 65ºC to fall again afterwards. The same applies for Tribolub-3 as viscosity peaks at 30ºC falls to 40,000 cP at 55ºC and smoothly rises again. The shear rate was 0.145 s-1.
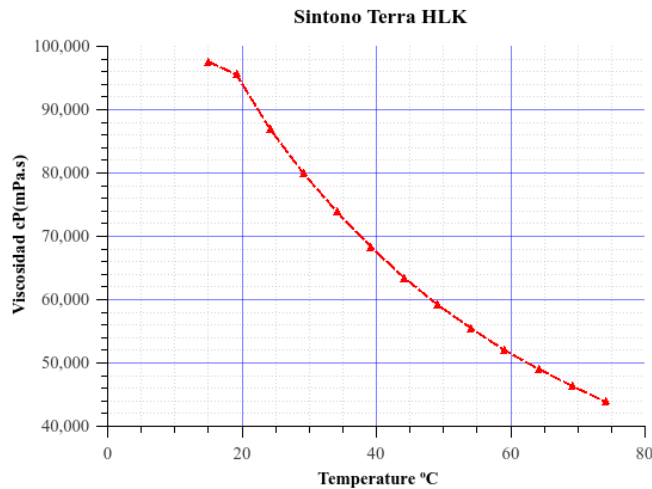
Figure 8.3: Sintono Terra HLK temperature curve.

Viscosity-temperature curve for Sintono Terra HLK shows a linear behavior as expected. Viscosity values fall from 100,000 Cp at 15ºC to 45,000 Cp near 70ºC.

8.1.2 Viscosity - time curves
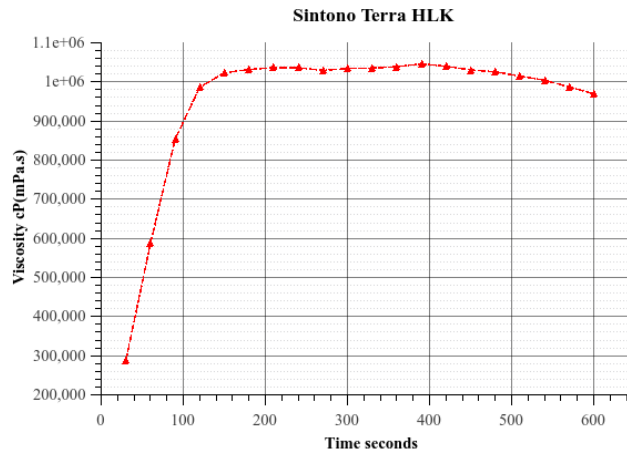
Figure 8.4: Sintono Terra HLK Viscosity- time curve.

Viscosity-time curve at a low shear rate for Sintono Terra HLK shows a rheopectic behavior that reaches values as high as 1 million cP that could have an incidence in its performance and is the possible explanation for the cloaks and obstructions in the lubrication system. Shear rate applied was 0.029 s-1 at 0.5 RPM to simulate stationary conditions.
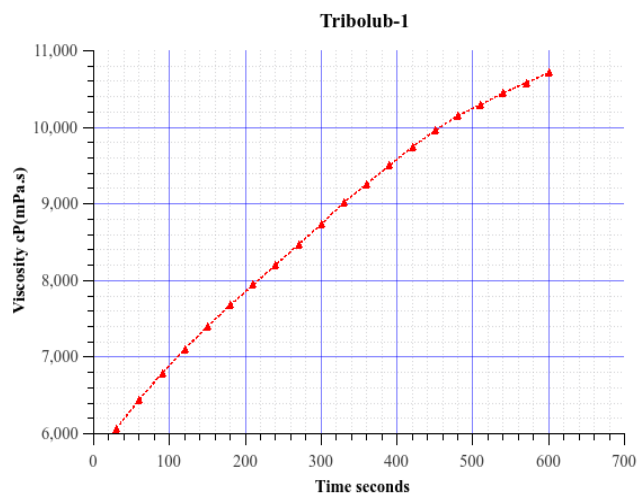
Figure 8.5: Tribolub-1 Viscosity-time curve.

Viscosity-time curve for Tribolub-1, a rheopectic behavior is clearly visible as seen in laboratory before when left static. Viscosity ranges from 6,000 cP at the beginning and almost doubles with values of 10,500 cP at 10 minutes. Shear rate 2.9 s-1 at 10RPM.
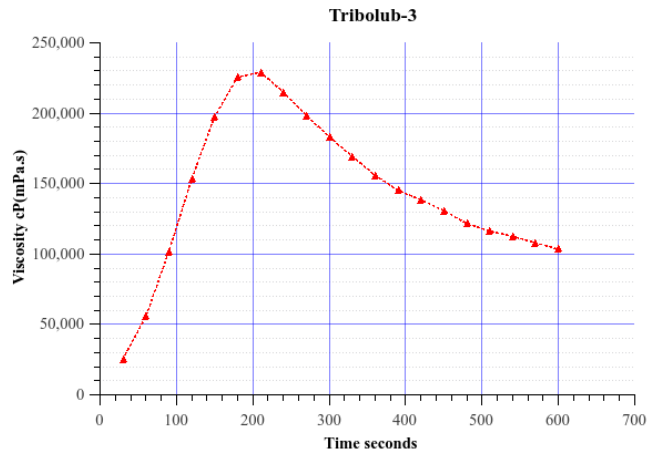
Figure 8.6: Tribolub-3 Viscosity-time curve.

Viscosity-time curve for Tribolub-3, a rheopectic behavior is clearly visible as seen both in field and laboratory before when left static. Viscosity ranges from 10,000 cP at the beginning and increases steadily to reach values of 230,000 cP at 200 seconds. Shear rate 2.9 s-1 at 10RPM.

Viscosity-speed curves for Tribolub-1 and 3 obtained using a LV4 spindle gave results regarding tendency and viscosity values, later confirmed by the rehometer.

8.1.3 Shear stress-shear rate/ Viscosity-shear rate curves
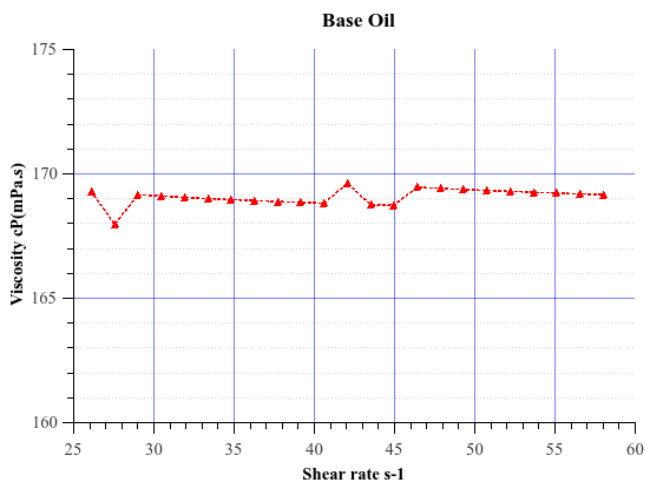
Figure 8.7: Base oil Viscosity-shear rate curve.
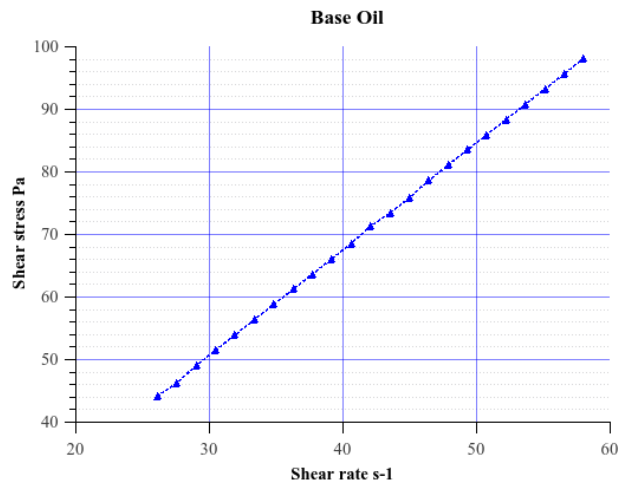
Figure 8.8: Base oil Shear stress-shear rate curve.

Viscosity remains almost constant for Tribolub base oil as shown in the graph ranging from 168 to 170 cP. Therefore it was possible to take a single point viscosity value. As seen in Shear stress-shear rate

curve, Tribolub base oil shows a newtonian behavior as corroborated by the Shear stress-shear rate curve.
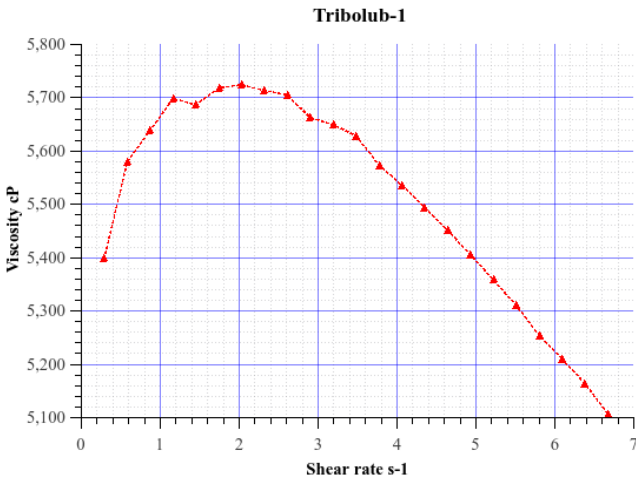
Figure 8.9: Tribolub-1 Viscosity-shear rate curve.
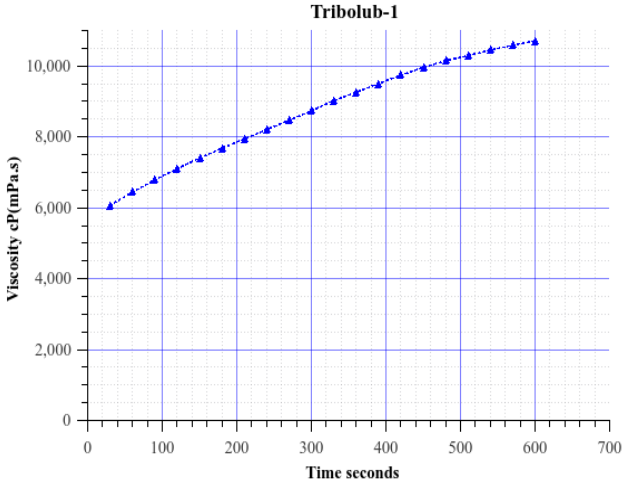
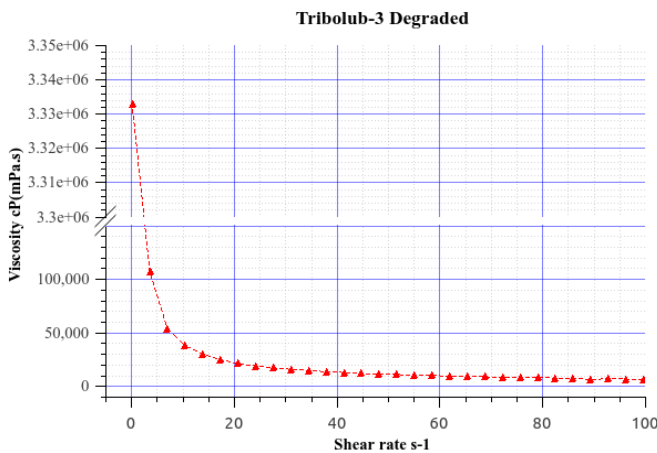**Figure 8.10: Tribolub-2 Shear stress-shear rate curve.**

Viscosity-shear rate curve for Tribolub-1 for low shear rate values ranging from 0.1 to 6.8 s⁻1. From 0.1 to 3 s-1 an increasing viscosity appears before it gives way to a shear-thinning behavior.
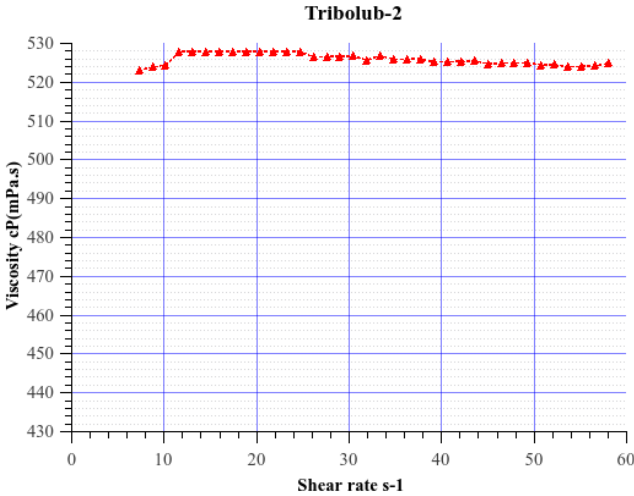
Figure 8.11: Tribolub-2 Viscosity-shear rate curve.
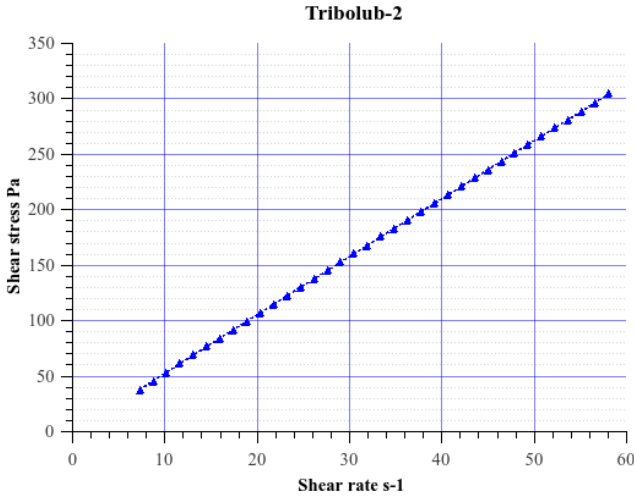
Figure 8.12: Tribolub-2 Shear stress-shear rate curve.

Tribolub-2 shows a newtonian behavior as could be seen in the shear stress vs shear rate curve.

Similar to Sintono Terra HLK Viscosity-time curve for Tribolub-3 shows a rheopectic behavior

46

increasing its viscosity ramp that goes from 10,000 up to 240,000 cP and falls again.
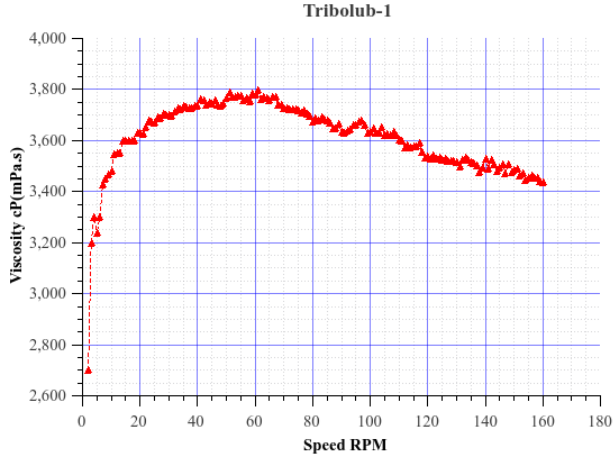
Figure 8.13: Tribolub-1 Viscosity-speed curve.
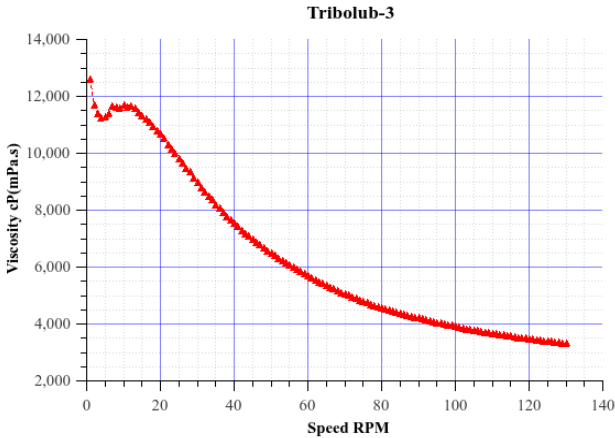
Figure 8.14: Tribolub-3 Viscosity-speed curve.

Tribolub-1 showed increasing values for low RPM to give way to a shear-thinning behaviour. Meanwhile, for Tribolub-3, a shear-thinning behavior is shown from 20 RPM on. However at lower speeds a particular behavior appears as seen in a viscosity increase. Relative Brookfield viscosity values for this sample ranged from 13,000 to 2,500 cP. Viscosity-speed curve for Sintono Terra HLK using LV4 spindle is shown in figure 8.15 below..
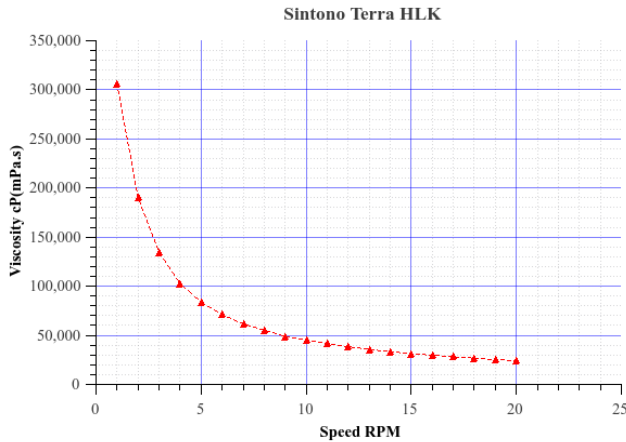
Figure 8.15: Sintono Terra HLK Viscosity-speed curve.
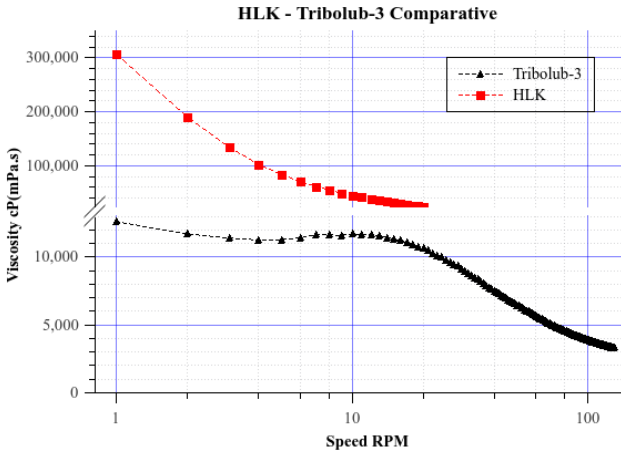
Figure 8.16: Tribolub-3 Viscosity-speed.

A shear-thinning behavior was confirmed as it is clearly visible with increasing speed. Viscosity values fall from 300,000 cP at low speed to nearly 20,000 at 20 RPM.

A viscosity-speed comparative curve is shown in figure 8.16, for Sintono Terra HLK and Tribolub-3 from 1 to 130 RPM using an LV4 spindle.

8.1.4 Up - down shear rate curves

The Up-down curves for Tribolub-3 at 25 and 40ºC show some differences in rheological behaviour
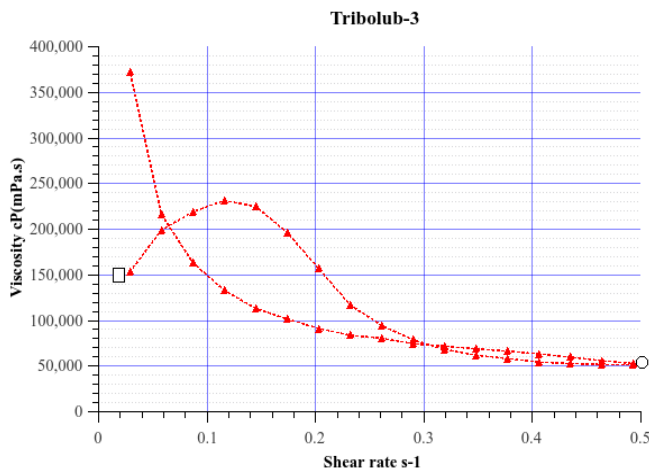
Figure 8.17: Tribolub-3 Up-down curve, 25ºC.   **Figure 8.18: Tribolub-3 Up-down curve, 40ºC.**
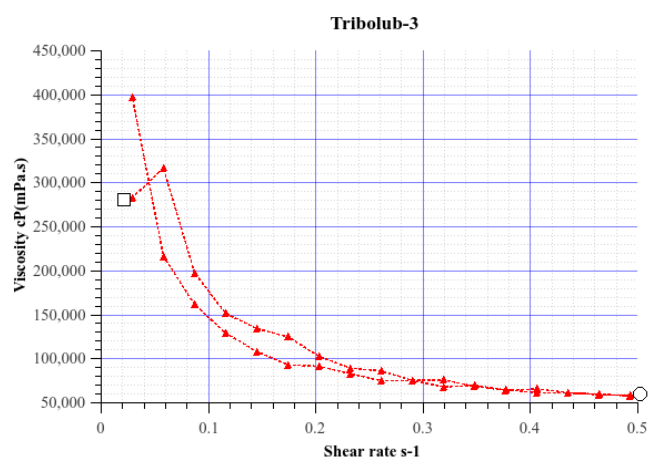
For the Up-down shear rate curve for Tribolub-3 at a temperature of 25 ºC. A particular behavior is shown in the graph. A shear thinning behavior for the lubricant is displayed though when reducing the shear rate after a maximum value, viscosity increases lightly in certain ranges. The ramp ending is marked with a square and the maximum shear rate attained is indicated using a circle.

In the case of the Up-down shear rate curves for Tribolub-3 at 40ºC, similar behavior as observed for room temperature is shown in the graph. A shear thinning behavior for the lubricant is displayed though when reducing the shear rate after a maximum value, viscosity increases just lightly in the ranges from 0 to 0.3 s-1.

8.2 Rheometric tests
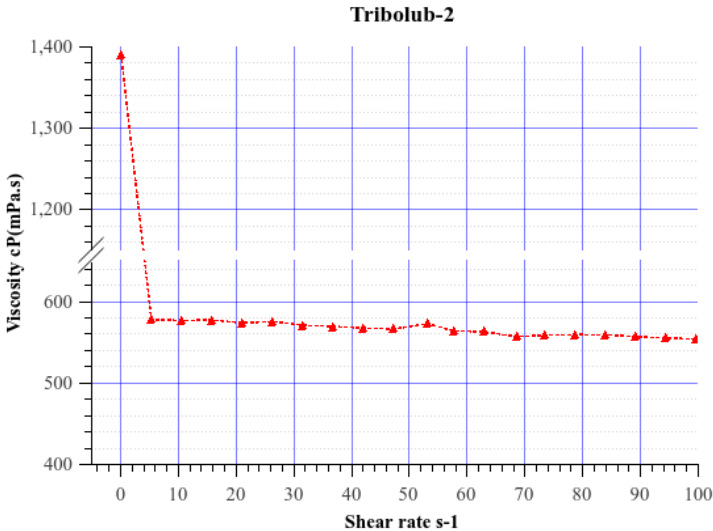
Figure 8.19: Tribolub-2 Viscosity-shear rate curve.

Viscosity-shear rate rheogram for Tribolub-2. Newtonian behavior is clearly seen for this lubricant making possible to have a single point viscosity of 580 cP.
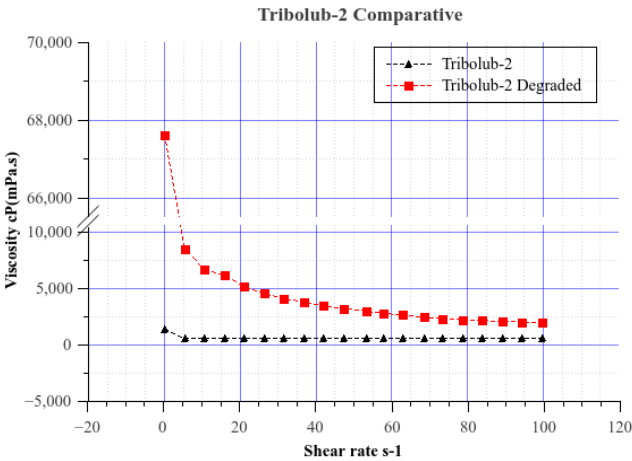
Figure 8.20: Tribolub-2 comparative Viscosity-shear rate curve.
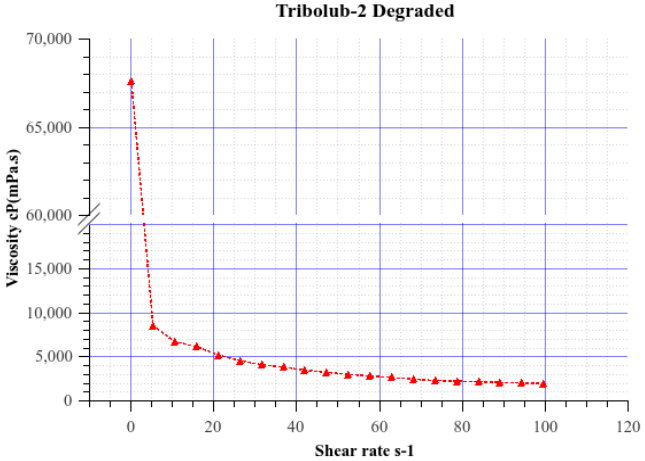
Figure 8.21: Tribolub-2 Viscosity-shear rate curve.

Tribolub-2 shows an increase in viscosity after undergoing degradation through twin disc testing. Values ranging from 1,000 up to 70,000 cP. With increasing shear rate degraded Tribolub-2 displays a shear-thinning behavior as it does before degradation. Both rheograms also show higher viscosity values for lower shear rate values which was previously suspected using the viscometer.

49
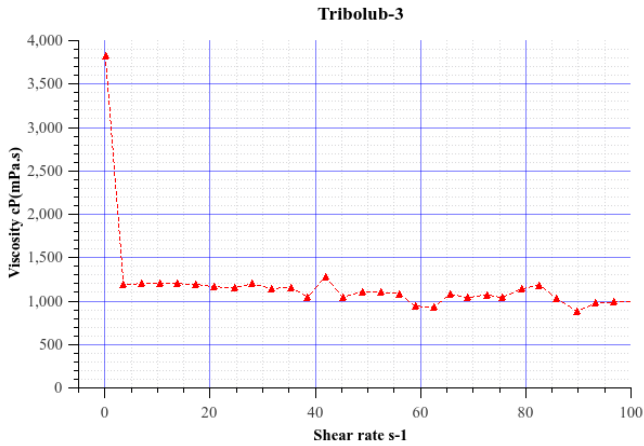
Figure 8.22: Tribolub-3 Viscosity-shear rate curve.
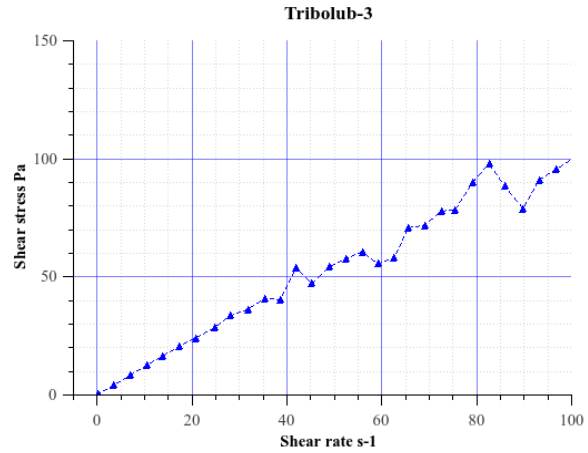
Figure 8.23: Tribolub-3 Shear stress-shear rate curve.

Viscosity-shear rate and Shear stress-shear rate curve for Tribolub-3 are shown above. A shear-thinning behavior was confirmed with viscosity values below 400,000 cP at low shear rates and below 1,000 cP for higher shear rates.

Figure 8.24: Degraded Tribolub-3 Viscosity-shear rate curve.
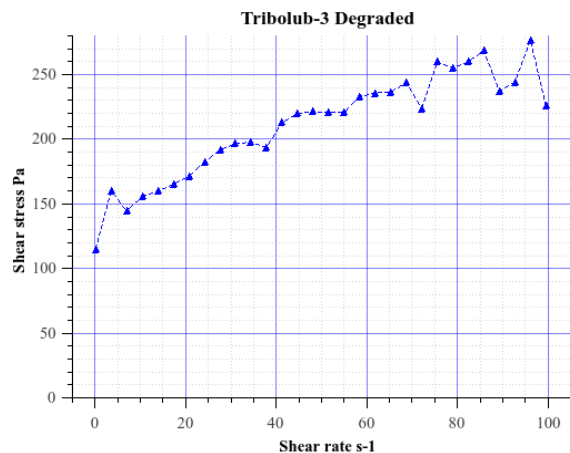
Figure 8.25: Degraded Tribolub-3 Shear stress-shear rate curve.

Above, Viscosity-shear rate and Shear stress-shear rate curve for degraded Tribolub-3, show that shear-thinning behavior was maintained but with an increase in viscosity as it was observed in values as high as 1,4 million cP, displayed for low shear rates.
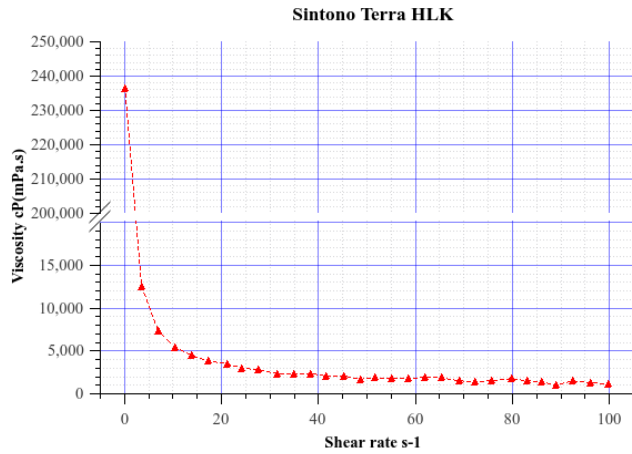
Figure 8.26: Sintono Terra HLK Viscosity-shear rate curve.
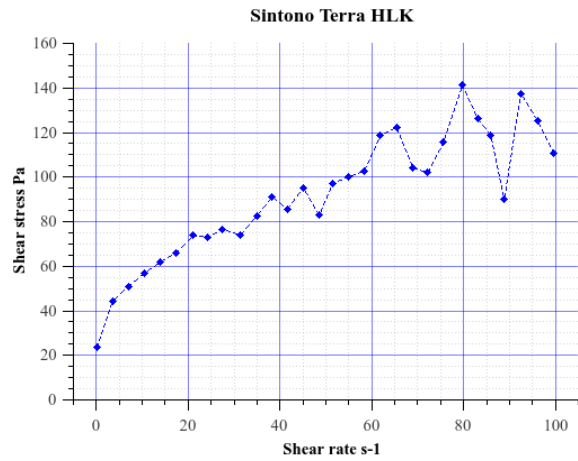
Figure 8.27: Sintono Terra HLK Shear stress-shear rate curve.

Viscosity-shear rate and Shear stress-shear rate curve for Sintono Terra HLK. Shear-thinning behavior is clearly seen with viscosity values ranging from 100,000 cP at low shear rates to 1,000 cP for higher rates.
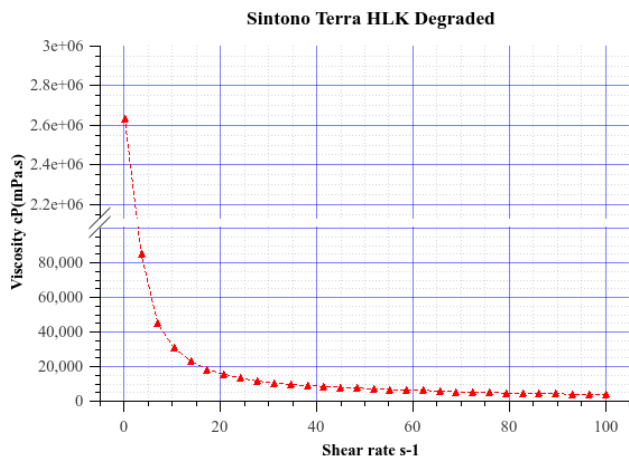
Figure 8.28: Degraded Sintono Terra HLK Viscosity-shear rate curve.
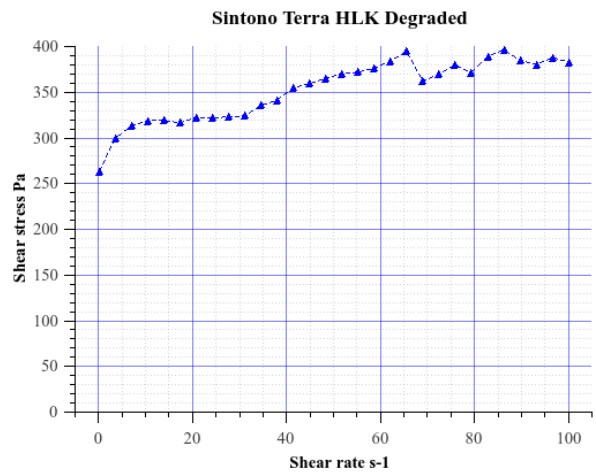
Figure 8.29: Degraded Sintono Terra HLK Shear stress-shear rate curve.

Viscosity-shear rate curve for degraded Sintono Terra HLK. Shear-thinning behavior is also seen in this curve and a considerable increase in viscosity compared with the curve before. Viscosity values range from 4 million cP to 1,000 cP

8.3 Wettability measurements
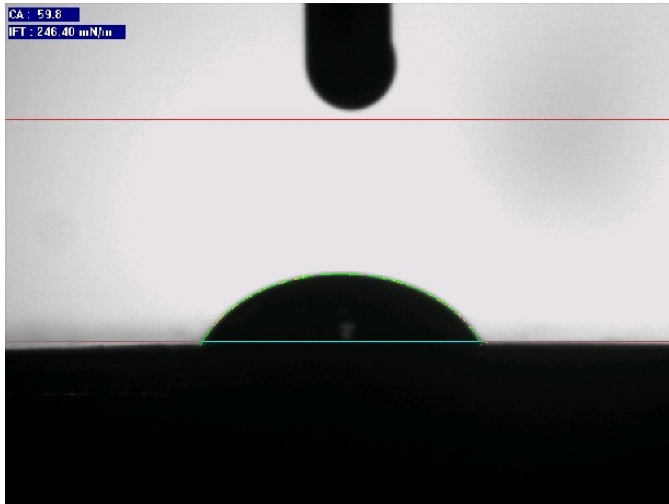
Figure 8.30: Tribolub wettability.

Tribolub-1 wettability test shows a contact angle of 59.8º and a brief period required -2.3 seconds- to obtain and stable lubricant droplet.
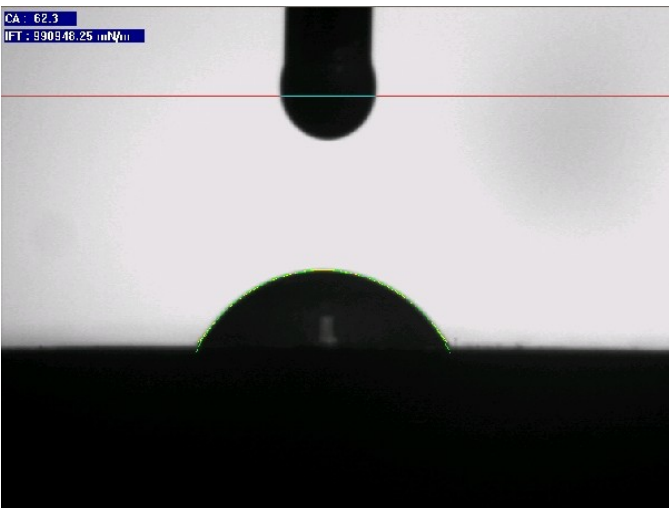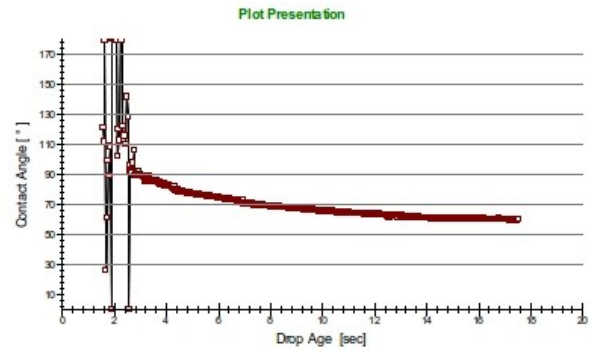
Figure 8.31: HLK-Locolub mixture wettability.

Wettability test for HLK-Locolub 50% mixture. A contact angle of 63.2º was obtained due to its higher viscosity and a longer stabilization time was required, 9.8 seconds in this case.
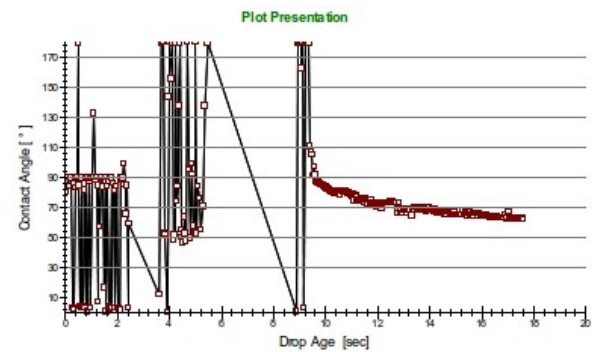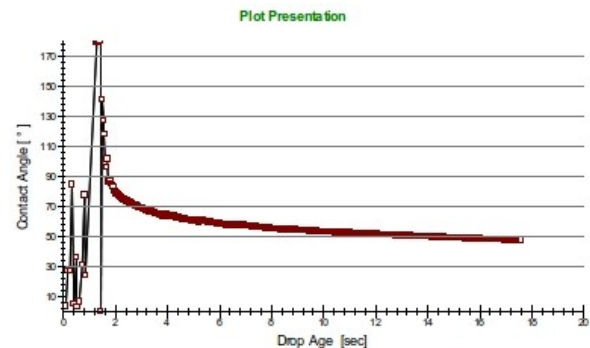
Figure 8.32: Locolub-Tribolub wettability.

Wettability test for a Locolub-Tribolub-1 50% mixture. A contact angle of 47.5º was obtained and a droplet stabilization time of 1.8 seconds due to its lower viscosity.

8.4 FTIR

Both Tribolub-3 and Sintono Terra HLK show several peaks at 2900, 1700, 1500, 1400, 1200, 1000 and 580 cm-1. The reason for these bands is related to the composition of each lubricant. The peaks 2908 cm-1 are related to the extension of C-H typical of saturated molecules. The signal at 3024 cm-1 corresponds to C-H extensions for unsaturated Carbon or aromatic molecules. The band appearing at 1727 cm-1 due to the stretching of C=O bonds and along with the band observed at 1224 cm-1, corresponding to C-O bonds stretching, prove the presence of an Ester functional group due to the nature of the based oil of both lubricants. For the signals at 1162 and 578 cm-1 their appearance is related to the nature of the grease which uses thickeners containing Si-O-Si bonds. An additional signal at 920 cm-1 also characteristic of Si-O bonds.
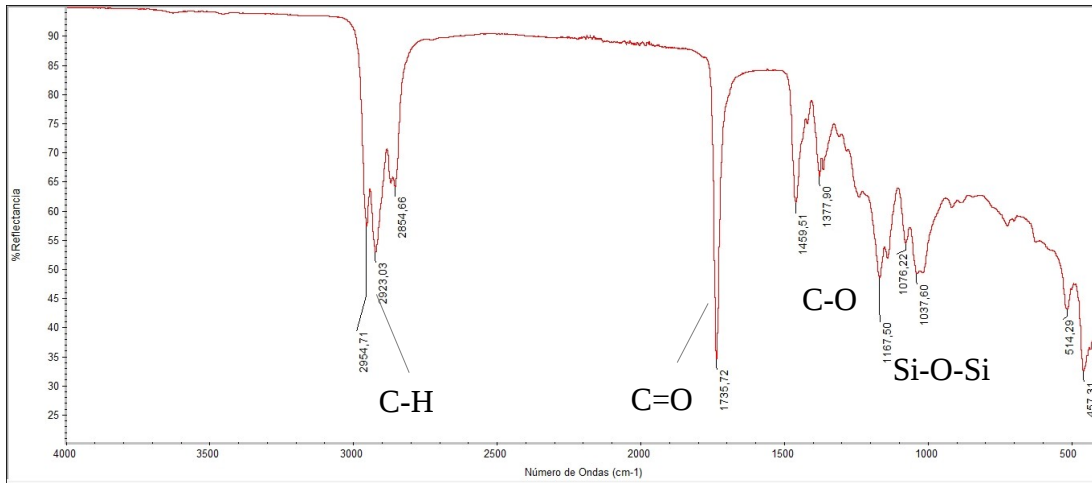
Figure 8.33: Sintono Terra HLK FTIR spectrum.

HLK spectrum shows several peaks at 2900, 1700, 1500, 1400, 1200, 1000 and 580 cm-1.

HLK degraded spectrum shows the same peaks shown for its non-degraded counterpart at 2900, 1700, 1500, 1400, 1200, 1000 and 580 cm-1. An increase of intensity for the peak at 1,900 cm-1 is observed compared to the non-degraded sample. In addition as slight change is seen for the peak at 2,900 cm-1. A change is observed in peaks related to C–H bond, 2850–3000 cm-1. These bands are related to CH_3 and CH_2 in aliphatic chains.
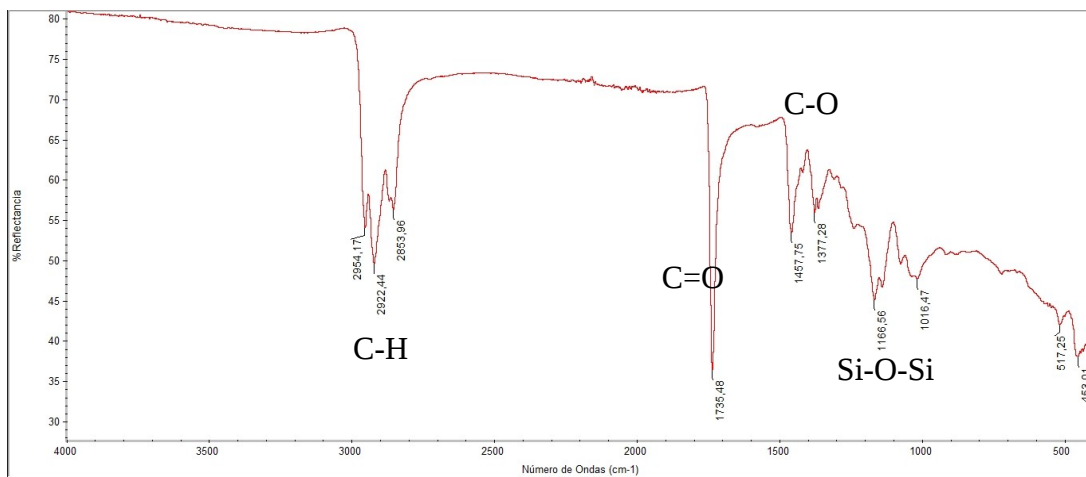
Figure 8.34: Degraded Sintono Terra HLK FTIR spectrum.

Tribolub-3 sample shows several peaks at 2,900, 1700, 1400, 1200, 700 and 480 cm-1.
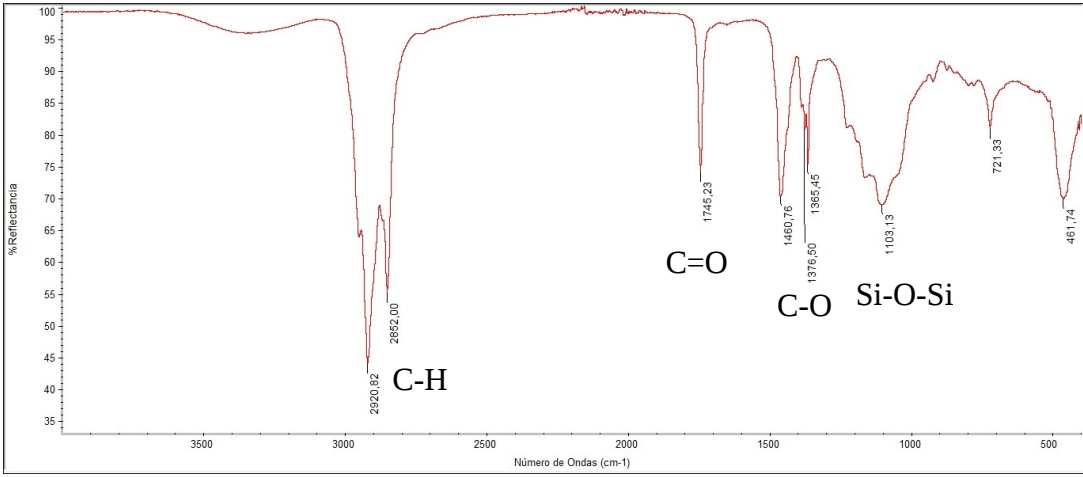
Figure 8.35: Degraded Tribolub-3 FTIR spectrum.

Tribolub-3 degraded sample shows considerable changes compared to its non-degraded counterpart, for the peaks at 2,900, 1700 and 1400 cm-1 a decrease is appreciated. For the ones at 1200, 700 and 480 cm-1 a slight increase is observed. A consequence of the oxidation is the change observed in the region of 1750–1700 cm-1. In this region CaO bond absorbs strongly, due to its large change in dipole moment.
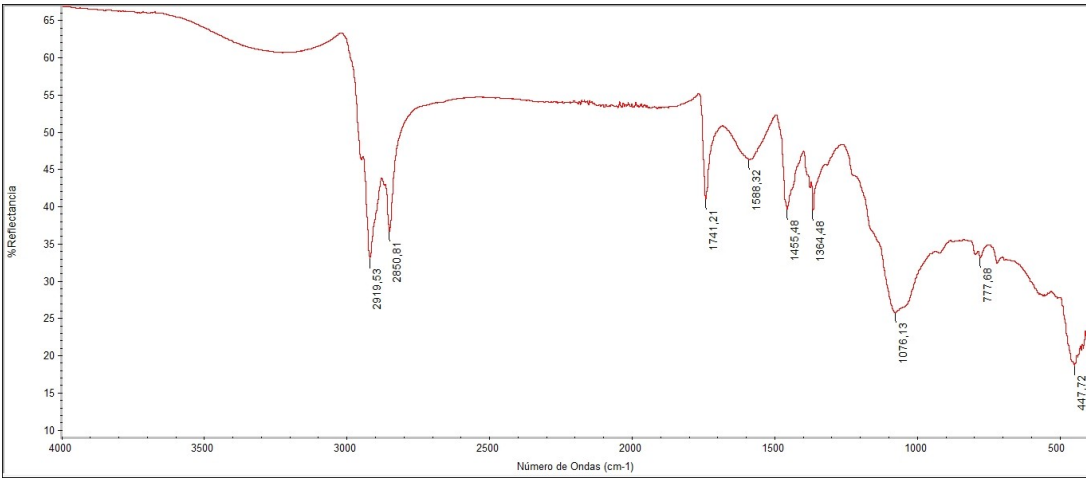
Figure 8.36: Degraded Tribolub-3 FTIR spectrum.
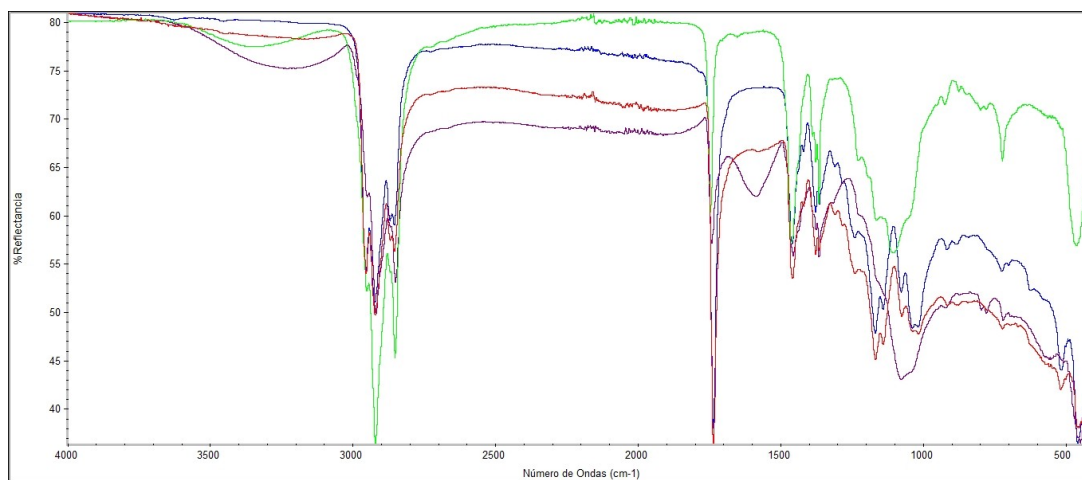
Figure 8.37: Comparative spectrum before and after degradation.

Figure 8.36 shows a comparative of spectrums obtained, oxidation is appreciated by an important increase in the area under the curve for the subsequent degraded samples. A posible nitration is also seen in the range of 1500-1700 cm-1 for Tribolub-3. A consequence of the oxidation is the change observed in the region of 1750–1700 cm-1.

In these spectra, bands at 1710 cm-1, which appear after mechanical degradation, are related to ketones, and it is also justified by the change in bands at 1471, 1450 cm-1 (aliphatic CH_3 and asymmetric CH_3 in alkenes) and1462 cm-1(CH_3, a functional group present in ketones and esters) and also by the enlargement of the band at 1157 cm-1 (C–C of alkanes), as a consequence of the presence of ketones and alkyl esters characteristic groups bonded to these carbons, by axial and angular deformation, C–C(=O)–C (ketones) and C–C(=O)–O (esters).

In the case of bands found between 1000 and 800 cm-1, these are related to C–C bonds. These bands are usually weak, thus broad OH bands due to carboxylic acid are usually overlapped.

Therefore, FTIR results indicate that lubricant degradation occurs by oxidation reactions, in agreement to literature results, probably leading to the formation of carboxylic acids and ketones .

8.5 Degradation tests

8.5.1 Tribological tests

Tribological tests performed using the Twin-disc machine show differences in performance for Sintono Terra and Tribolub-3 lubricants. Differences in stabilization time, friction coefficients and wear parameters.

HLK
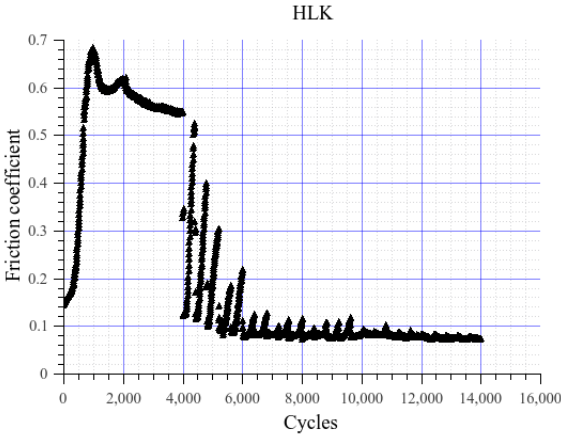
**Figure 8.38: Degraded Sintono Terra
HLK friction coefficient curve.**

Friction coefficients for degraded Sintono Terra HLK. Stabilization was reached until 9,000 cycles, from this value on small variations are seen due to an increase viscosity and low wettability of this degraded lubricant.
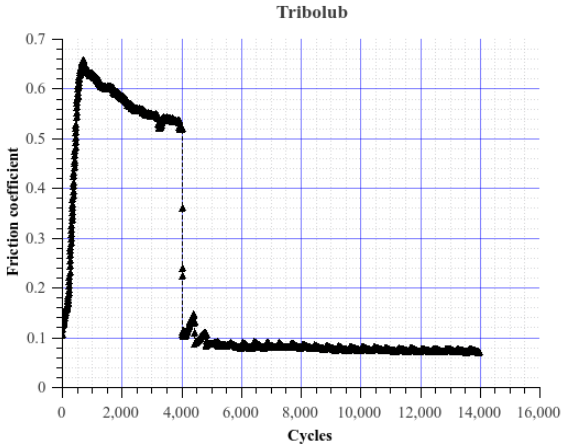
Tribolub

**Figure 8.39: Tribolub-3 friction
coefficient curve.**

Friction coefficient curve for Tribolub-3. Stabilization was reach until 5,000 cycles.
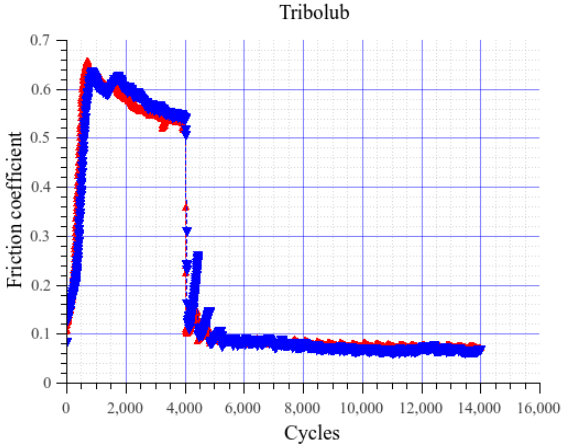
**Figure 8.40: Tribolub-3 comparative
friction coefficient curve.**

Friction coefficient comparative curve, red Tribolub-3 before suffering degradation, blue after degradation process in the Twin-disc test. Degraded Tribolub-3 is slighty below its non-degraded counterpart.
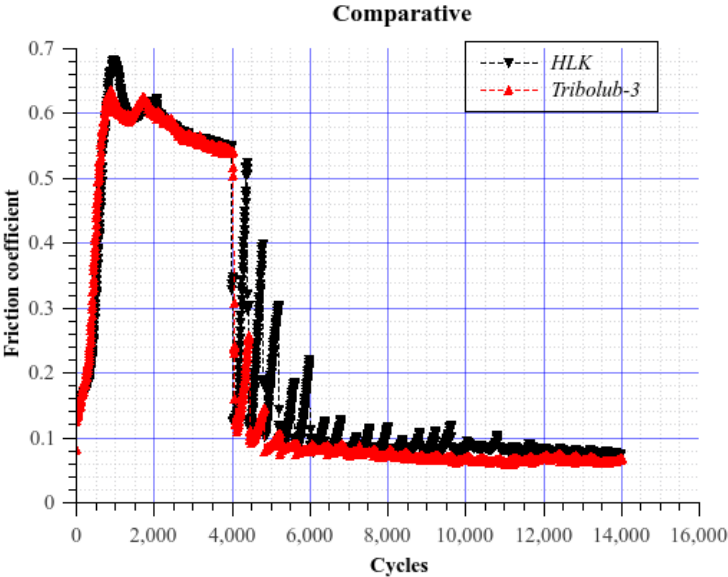
**Figure 8.41: Tribolub-3 – HLK degraded samples
comparative friction coefficient curve.**

Comparative curve of friction coefficients for both degraded Tribolub-3 and Sintono Terra HLK. A remarkable difference is seen regarding stabilization time and friction coefficient values being higher

for the degraded sample.
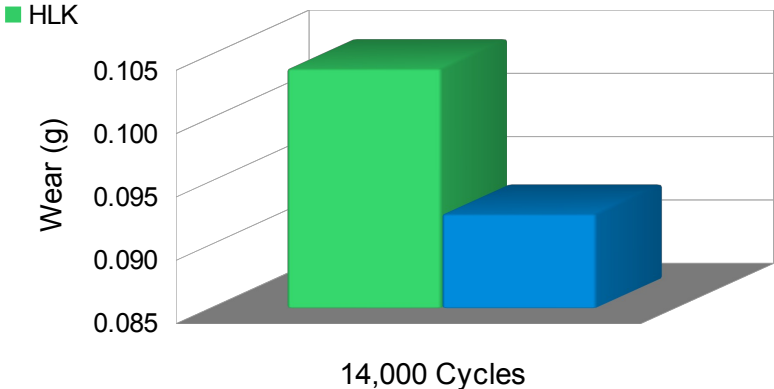
Figure 8.42: Average wear.

Wheel-rail average wear chart for degraded Sintono Terra HLK and Tribolub-3. A higher wear is appreciated for degraded Sintono Terra HLK.
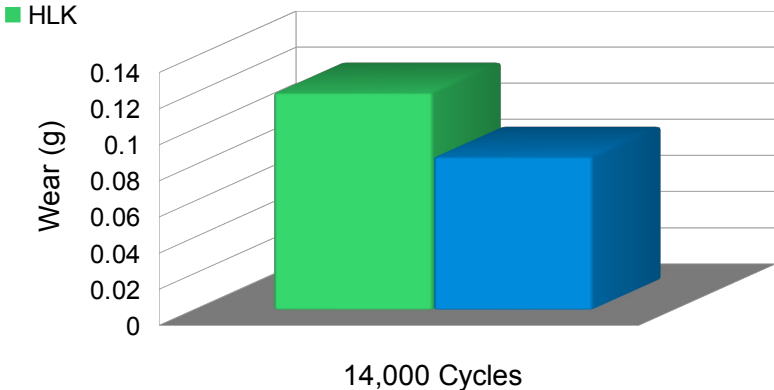
Figure 8.43: Rail average wear.

Rail average wear chart for degraded Sintono Terra HLK and Tribolub-3. A higher wear is appreciated for degraded Sintono Terra HLK.
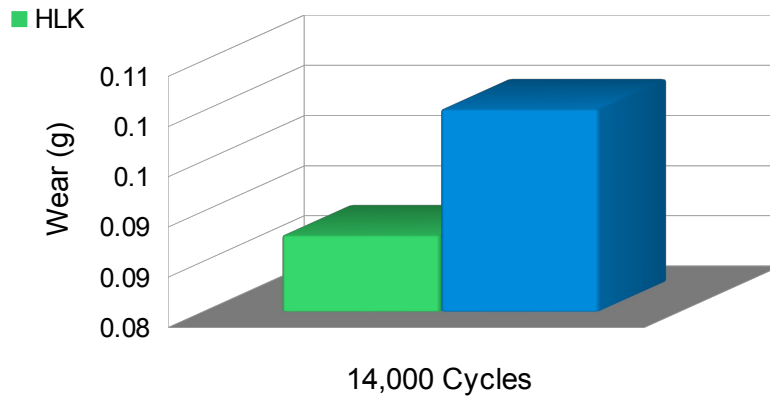
Figure 8.44: Wheel average wear.

Wheel average wear chart for degraded Sintono Terra HLK and Tribolub-3. An opposite behavior is observed as a higher wear is appreciated for degraded Tribolub-3 in this case.

8.5.2 Photodegradation

Photodegradation samples chosen for analysis, using a rheometer were exposed to 48 hours of degradation process simulating solar radiation.

Sintono Terra HLK was not severely affected by photodegradation. Viscosity-shear rate and Shear stress-shear rate curve for photodegraded Sintono Terra HLK showed a shear thinning behavior with values as high as almost 16,000 cP at low shear rates as observed in viscometric tests before. It is noteworthy to mention that instead of increasing its viscosity it slightly decreased for low shear rate values.
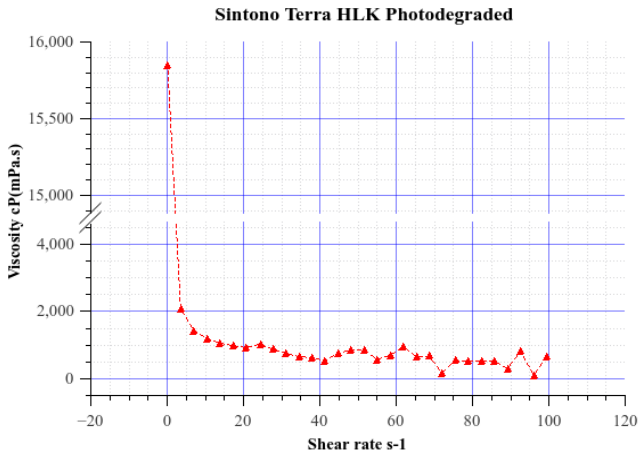
Figure 8.45: Photodegraded Sintono Terra HLK Viscosity-shear rate curve.
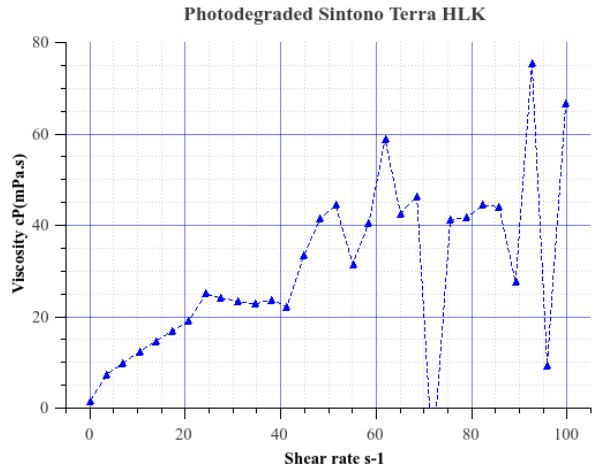
Figure 8.46: Photodegraded Sintono Terra HLK Shear stress-shear rate curve.

Viscosity values for Sintono Terra HLK ranged from 15,800 cP to values around 500 cP at high shear rates.

In the case of Tribolub and its predecessors, shear-thinning properties are maintained even after the degradation process.
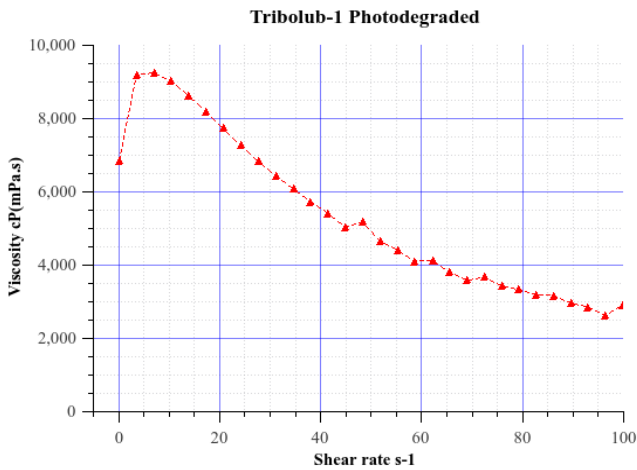
Figure 8.47: Photodegraded Tribolub-1 Viscosity-shear rate curve.
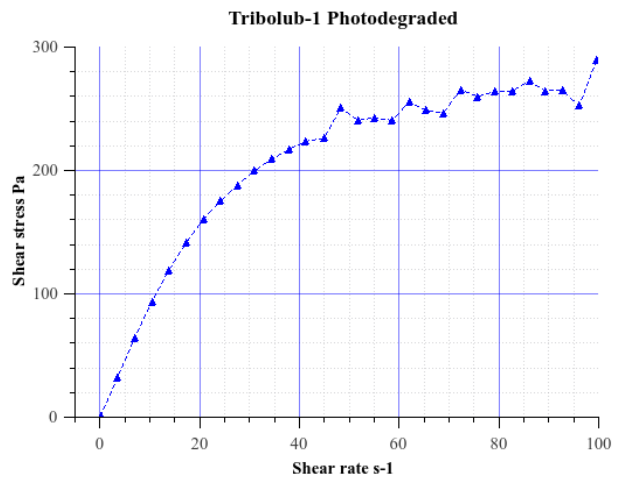
Figure 8.48: Photodegraded Tribolub-1 Shear-stress-shear rate curve.

For photodegraded Tribolub-1 viscosity ranges from 9,000 cP to 5,000 cP. From 0 to 10 s-1 the grease shows an increase in viscosity, a short shear-thickening segment, before falling again and displaying a shear-thinning behavior.
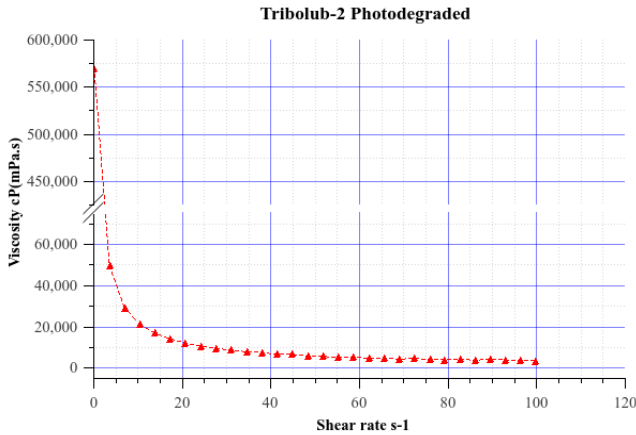
Figure 8.49: Photodegraded Tribolub-2 Viscosity-shear rate curve.
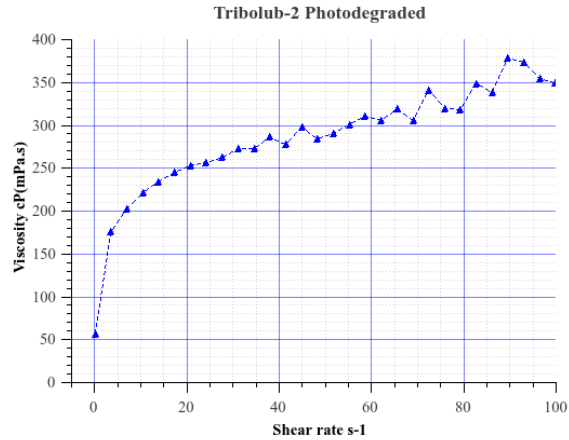
Figure 8.50: Photodegraded Tribolub-1 Shear-stress-shear rate curve.

Photodegraded Tribolub-2 displayed a shear-thinning behavior, viscosity varied from 570,000 cP to 5,000 cP with the increase in shear rate. This non-Newtonian behavior is due to polymerization effects that occur even though no Fe particles are available to catalyze the chemical degradation.
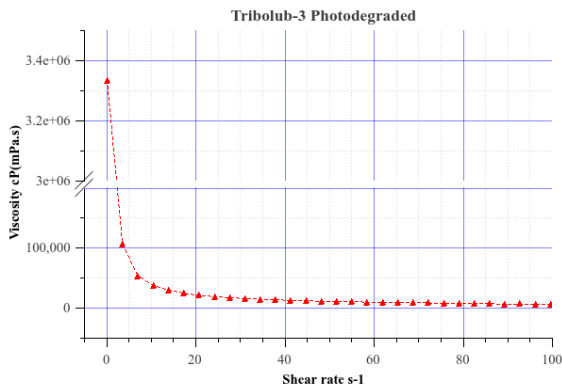
Figure 8.51: Photodegraded Tribolub-3 Viscosity-shear rate curve.
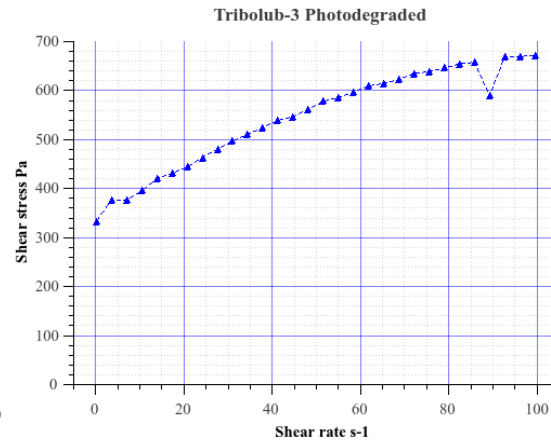
Figure 8.52: Photodegraded Tribolub-3 Shear stress-shear rate curve.

For photodegraded Tribolub-3, viscosity increases from an interval of 400,000-1,000 cP to a range from 3,3 million cP to 5,000 cP, and displaying a shear-thinning behavior.

8.6 *Optical Microscope*

A general overview of Sintono Terra HLK, Tribolub-3 and its degraded counterparts morphology was

obtained using an Optical Microscope. Differences in color, grain size and particle concentration were observed among the samples before and after degradation as seen in table 8.3 below..
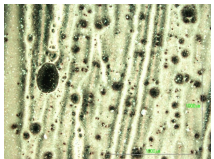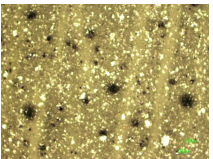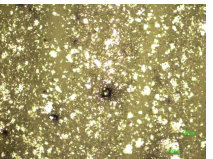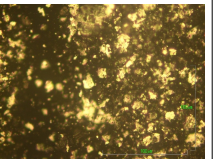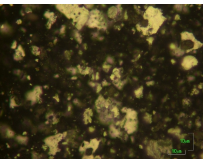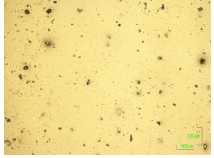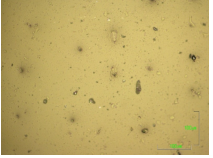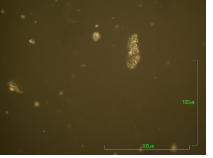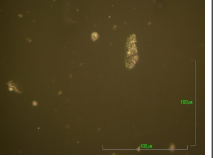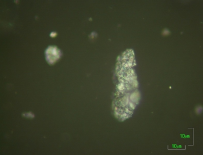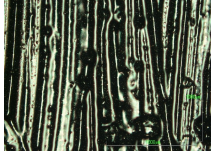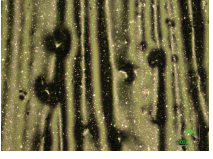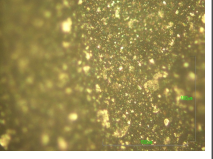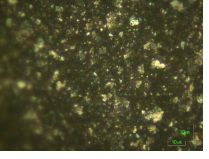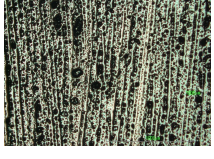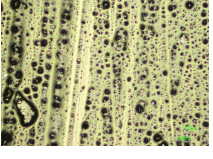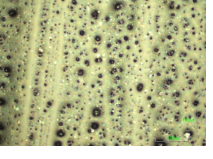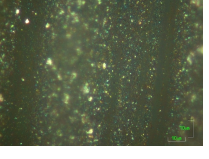
FM	5X	10X	20X	50X	100X
Sintono Terra HLK					
Tribolub-3					
Sintono Terra HLK (Degraded)					
Tribolub-3 (Degraded)					

Table 8.3

Micrographs taken at 50X for Sintono Terra HLK before and after degradation show a grain size reduction in the degraded sample product of the grinding phenomenon taking place at the wheel-rail system and changes in morphology are observed as some small flakes appear.

Micrographs at 5 and 10X for both degraded Sintono Terra HLK and Tribolub-3, show a darker appearance while at 100X Tribolub-3 shows a substantial increase of metallic particles product of wear during mechanical degradation. This increase in metallic particles is accountable for catalyzing the subsequent degradation along with pressure and temperature in the wheel-rail system.
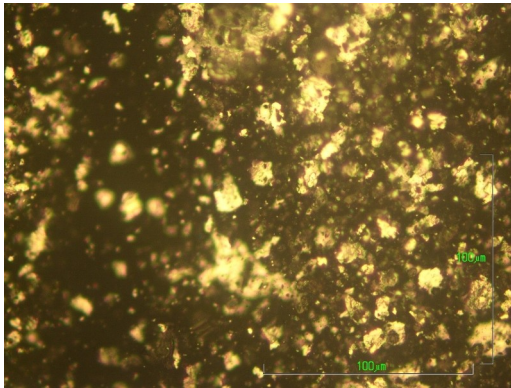
Figure 8.53: Sintono Terra HLK before degradation.   **Figure 8.54: Sintono Terra HLK after degradation.**
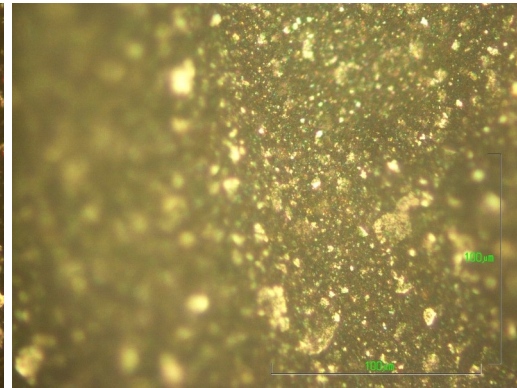
Generally speaking, particle size ranges between 10 and 25 µm before degradation while after the tests the predominant size is circa 10 µm. For Tribolub-3 below, a substantial increase of particle content is observed in detail as just few additive particles are visible before degradation.
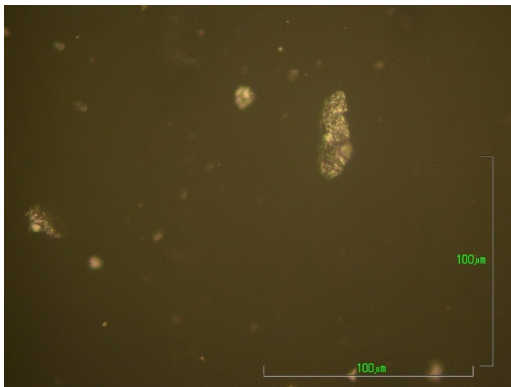
Figure 8.55: Tribolub-3 before mechanical degradation.   **Figure 8.56: Tribolub- 3 after mechanical degradation.**
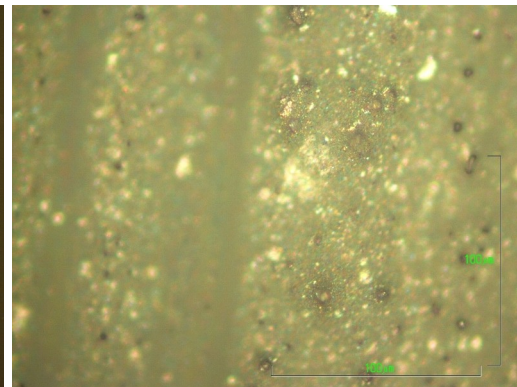
8.7 SEM

SEM micrographs confirmed initial observations obtained using a simple Optical microscope regarding particle content increase and some particular shapes with sizes ranging from 10 to 25 µm, found after mechanical degradation. The micrographs for Sintono Terra HLK before mechanical degradation process, at magnification of X500 and X750 are shown below.
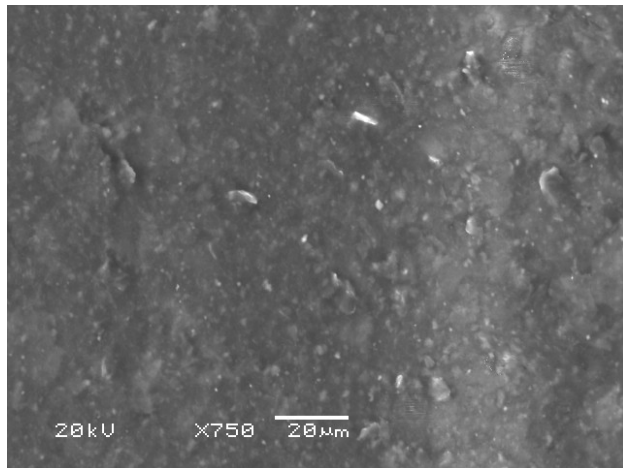
Figure 8.57: Sintono Terra HLK X750.
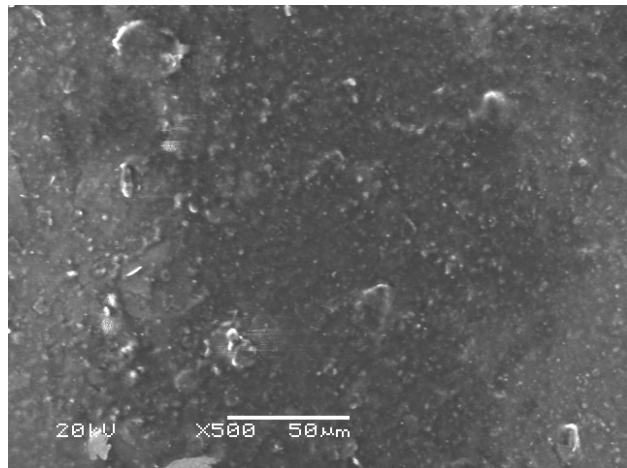
Figure 8.58: Sintono Terra HLK X500.

A homogeneous particle distribution is shown as was previously observed using an optical microscope.
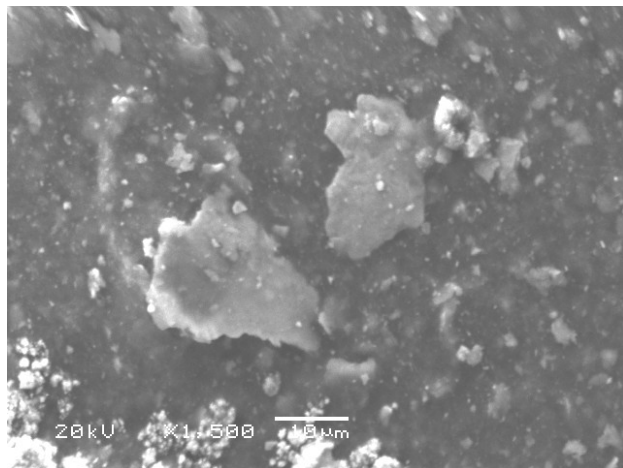
Figure 8.59: Degraded Sintono Terra HLK X1,500.
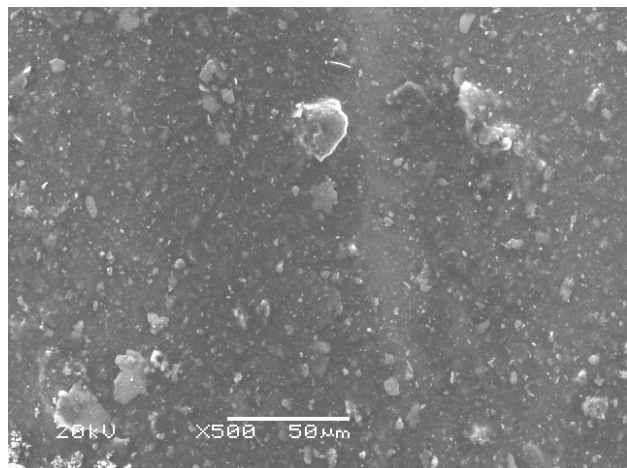
Figure 8.60: Degraged Sintono Terra HLK X500.

The SEM micrographs for degraded Sintono Terra HLK at X1,500 and X500, show an increase of particle content as previously observed. This confirms the presence of considerable amounts of particles produced by wear in the wheel-rail system and that have a potential as catalyst of the degradation process. In addition the appearance of certain flake shaped particles of great size is clearly seen.
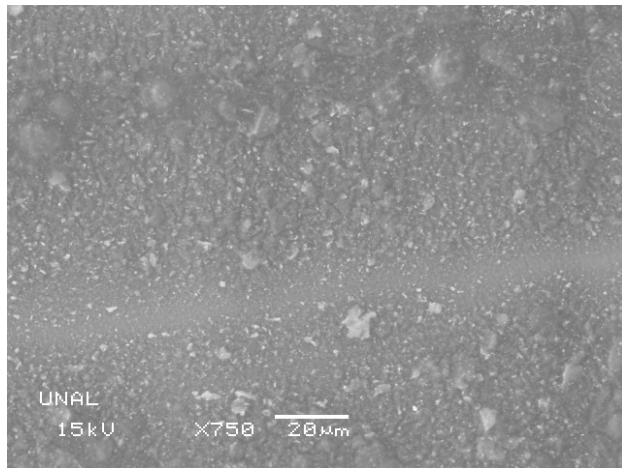
Figure 8.61: Tribolub-3 X750.
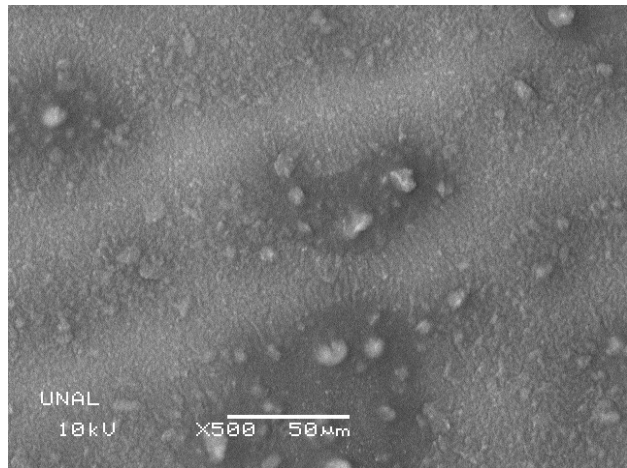
Figure 8.62: Tribolub-3 X500.

The SEM micrographs for Tribolub-3 before and after degradation, at X500 and X750, show the same trend as for HLK. First, homogeneous particle distribution is shown as observed using an optical microscope.
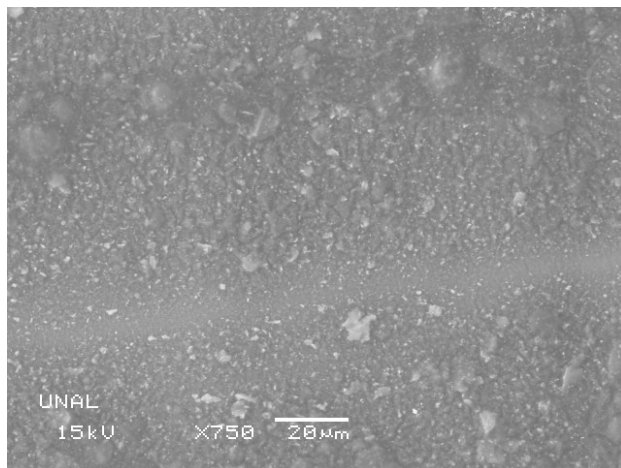
Figure 8.63: Degraded Tribolub-3 X750.
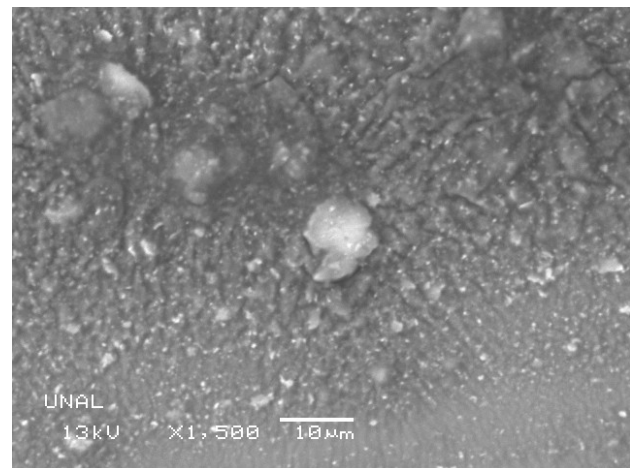
Figure 8.64: Degraded Tribolub-3 X1,500.

Later SEM micrographs for degraded Tribolub-3 at X1,500 and X500, show an increase of particle content. In addition the appearance of certain flake shaped particles of approximately 10 μm is again clearly seen.

8.7.1 EDXS analysis

EDXS analysis confirmed the presence of Fe particles as expected due to wear in the wheel-rail

system. Special attention was directed at the Flake shaped particles found on degraded Sintono Terra HLK using an Optical Microscope.
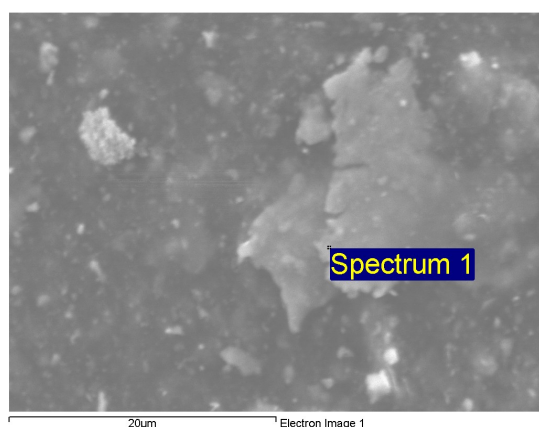
Figure 8.65: Particle analyzed on degraded Sintono Terra HLK.
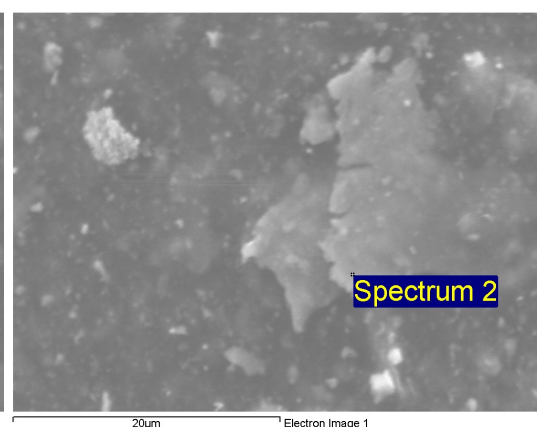
Figure 8.66: Second target of the particle analyzed.
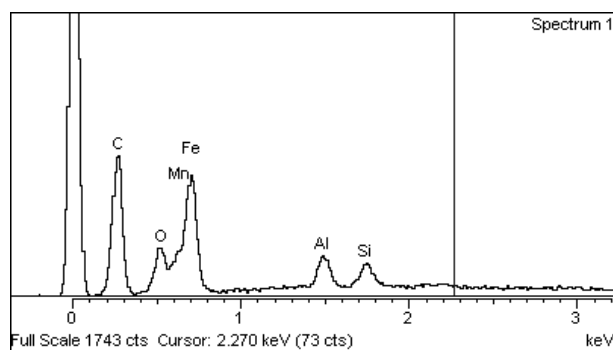
Figure 8.67: EDS spectrum for degraded Sintono Terra HLK.
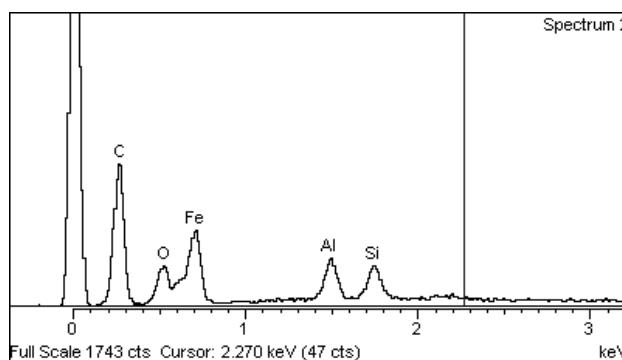
Figure 8.68: EDS spectrum for degraded Tribolub-3.

The table below lists concentrations found in degraded Sintono Terra HLK for each element described:

Element	Weight %	Atomic %	Element	Weight %	Atomic %
C K	42.66	69.32	C K	48.54	71.56
O K	10.87	13.26	O K	13.34	14.76
Al K	2.01	1.45	Al K	2.75	1.80
Si K	1.21	0.84	Si K	2.08	1.31
Mn K	0.59	0.21	Fe K	33.31	10.56
Fe K	42.66	14.91	Totals	100.00	
Totals	100.00				

Table 8.4.1

Fe as shown above is a predominant element found on degraded Sintono Terra HLK.
Figure 8.68 and 8.69 below, show particles analyzed embed in degraded Tribolub-3.
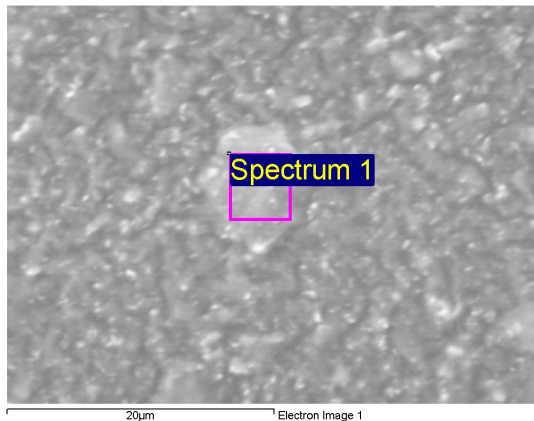
Figure 8.69: Section analyzed form
degraded Tribolub-3.

Figure 8.70: Particle analyzed from
degraded Tribolub-3.

The following table below list element composition for degraded Tribolub-3 according to their weight and quantities present:

Element	Weight %	Atomic %	Element	Weight %	Atomic %
C K	49.16	80.58	C K	59.01	78.91
O K	3.05	3.75	O K	12.01	12.06
Al K	0.33	0.24	Al K	1.15	0.68
Si K	1.08	0.76	Si K	4.00	2.29
Mn K	0.77	0.28	Ca K	0.59	0.24
Fe K	38.93	13.72	Fe K	19.05	5.48
Totals	100.00		Au M	4.19	0.34
			Totals	100.00	

Table 8.4.2

Elements found on both samples are consistent with each lubricant composition and products obtained from wear of the wheel-rail system. Chemical elements such as; Ca, Si and Al are additives with an specific purpose while Fe was a predominant element on both degraded samples with considerable amounts to have a significant effect on activating chemical degradation reaction, although other metallic particles may play an important role as well.

9 Discussion

9.1.1 Rheological degradation indicators

Different mathematical models were fitted to the obtained rheograms; Herschel-Bulkely, Carreau and Sisko equations were fitted for greases and the parameters; σ_0 *yield stress,* k consistency index , n flow index, these were compared before and after degradation as shown in the table 9.1.1 below:

FM	σ_0 (Pa)	k	n	η_0 (Pa.s)	η_∞ (Pa.s)	Model
Sintono Terra HLK	-	34.5	0.6272	-	0.5824	Sisko
Tribolub-3	-	0.6689	0.621	-	1.017	Sisko
Sintono Terra HLK (Degraded)	-	278.9	0.9745	-	1.147	Sisko
Sintono Terra HLK (Photodegraded)	-	3.902	0.5999	-	0.2769	Sisko
Tribolub-3 (Degraded)	-	134.3	0.9341	-	10.45	Sisko
Tribolub-1 (Photodegraded)	-	2.274X10-4	2.18	8.58	1.604	Cross
Tribolub-2 (Photodegraded)	-	161.1	0.8703	933.3	-	Cross
Tribolub-3 (Photodegraded)	-	343	0.987	-	1.017	Sisko

Table 9.1.1: n < 1, the fluid exhibits shear-thinning properties, n = 1, the fluid shows Newtonian behavior and for n > 1, the fluid shows shear-thickening behavior.

Flow index values, show shear-thinning properties for both lubricants Tribolub-3 -including its previous versions- and Sintono Terra HLK and their degraded counterparts. This analysis also shows that Sisko and Cross rheological models were the best match for most of samples analyzed. Herschel-Bulkley model was discarded due to the non-linarity of the data as it was noted in by the negative yield point values obtained.

The consistency index, k, indicates how the lubricant behaves when it experiences low shear rates. The consistency index shows that Sintono Terra HLK and its degraded counterparts are very viscous at low shear rates while on the other hand Tribolub photodegraded samples also displayed the same trend and high viscosity values.

η_0 values obtained for Cross models show a polimerization during degradation process for both Tribolub and Sintono HLK samples, according with the Near-zero viscosity approach.

Figures below from 9.1-9.8 correspond to the corrected curves for Viscosity&shear stress – shear rate according to the mathematical model applied in each case Sisko or Cross.

Figure 9.1 and 9.2 correspond to the corrected curves for Viscosity&shear stress – shear rate for Sintono Terra HLK and Tribolub-3 before suffering degradation using a Sisko model.

Figure 9.1: Sintono Terra HLK Viscosity& Shear-stress-shear rate corrected curve.

Figure 9.2: Tribolub-3 Viscosity& Shear-stress-shear rate corrected curve.

Figure 9.3: Photodegraded Tribolub-1 Viscosity& Shear-stress-shear rate corrected curve.

Figure 9.4: Photodegraded Tribolub-2 Viscosity& Shear-stress-shear rate corrected curve.

From figure 9.3 to 9.6 above, we have the corrected curves for Viscosity&shear stress – shear rate for Sintono Terra HLK and Tribolub-3 after undergoing photodegradation. Tribolub-1 and -2 used a different model, Cross for each one while for the remainding, Sisko was again the best match.

Figure 9.5: Photodegraded HLK Viscosity& Shear-stress-shear rate corrected curve.
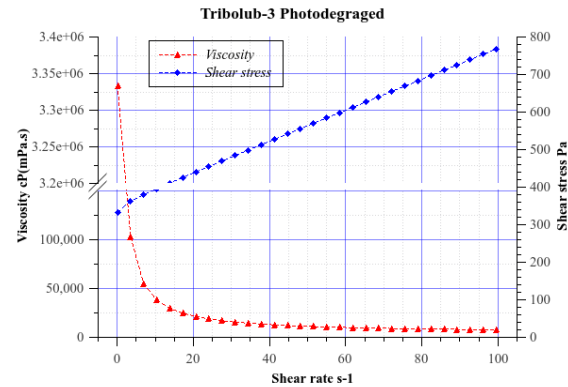
Figure 9.6: Photodegraded Tribolub-3 Viscosity& Shear-stress-shear rate corrected curve.

Finally, figure 9.7 and 9.8 below, account for the corrected curves for Viscosity&shear stress – shear rate for Sintono Terra HLK and Tribolub-3 after mechanical degradation sing the Twin-disc machine. Sisko was also suitable for these rheograms.
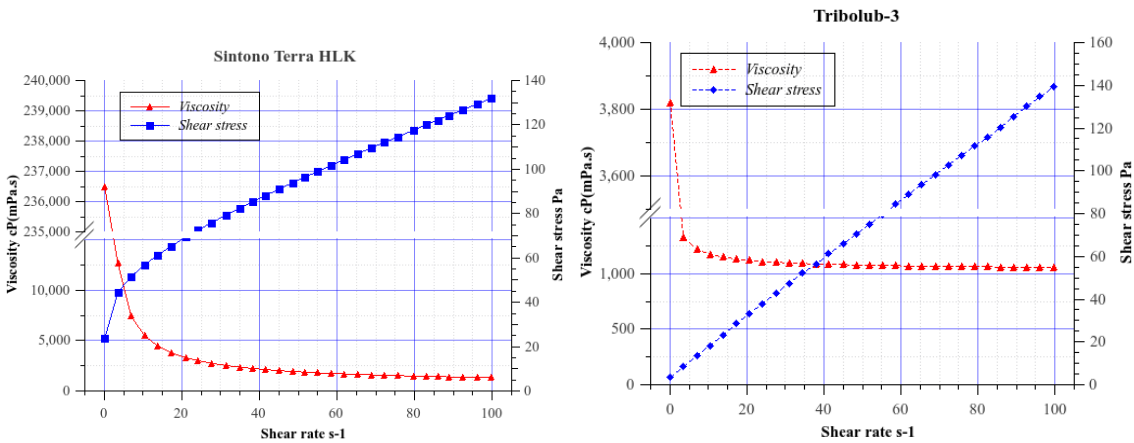

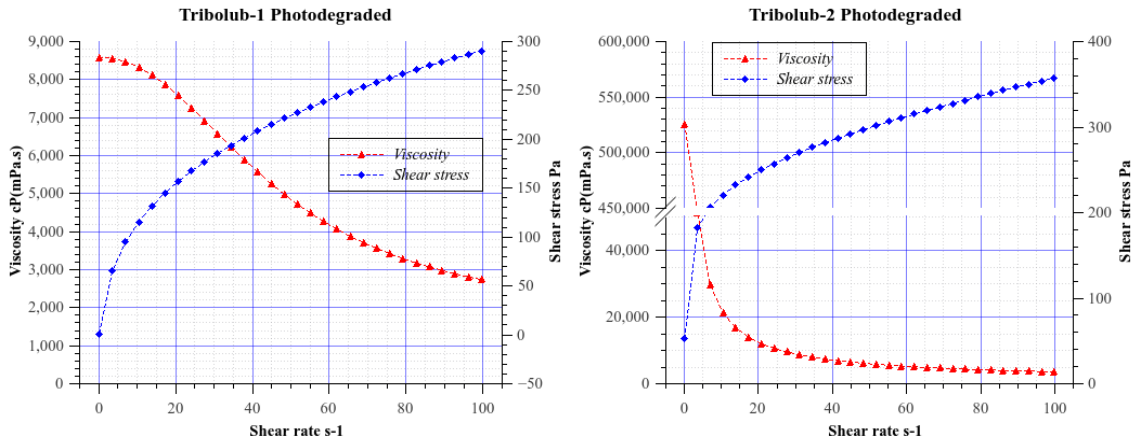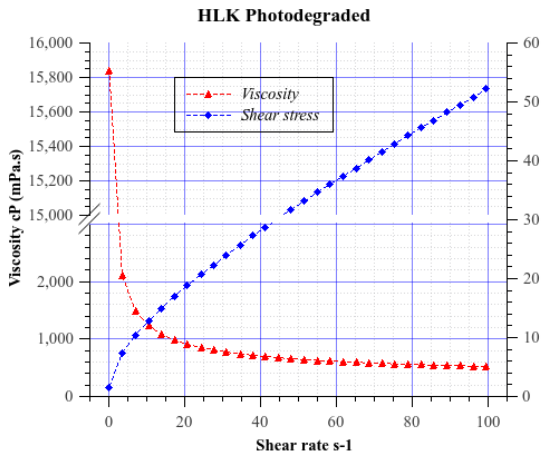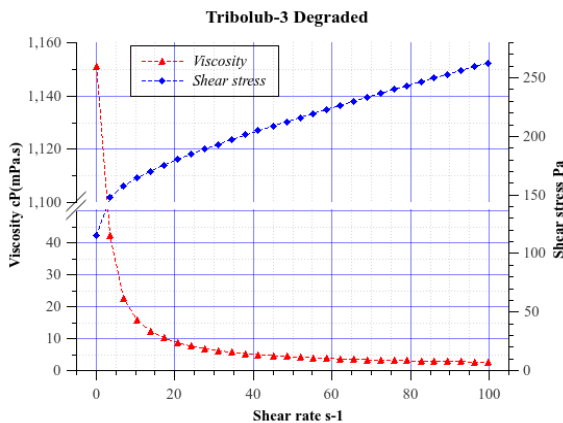**Figure 9.7: Degraded Tribolub-2 Viscosity& Shear-stress-shear rate corrected curve.**
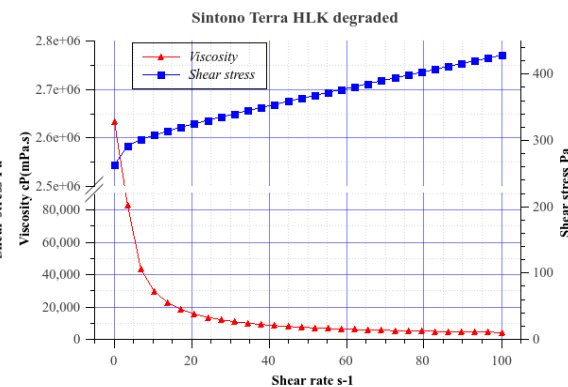

Figure 9.8: Degraded HLK Viscosity& Shear-stress-shear rate corrected curve.

The table below summarizes viscosity ranges found for each lubricant analyzed.

FM	*Viscosities cP(mPa.s)*	Model
Sintono Terra HLK	200,000 - 1,000	Sisko
Tribolub-1	9,000-3,000	No model

Tribolub-2	570	Newtonian flow
Tribolub-3	400,000 - 1,000	Sisko
Sintono Terra HLK (Degraded)	4 million - 1,000	Sisko
Sintono Terra HLK (Photodegraded)	15,800 - 500	Sisko
Tribolub-3 (Degraded)	1,4 million – 10,000	Sisko
Tribolub-1 (Photodegraded)	7,000 - 3,000	Cross
Tribolub-2 (Photodegraded)	570,000 – 3,500	Cross
Tribolub-3 (Photodegraded)	3,3 million – 6,750	Sisko

Table 9.1.2

Degraded lubricants by simulating the rail-wheel system show a considerable increase in viscosity while on the other hand the change produced by Photodegradation on each lubricant rheological properties was below mechanical degradation for Sintono Terra HLK while Tribolub and its predecessors were heavily affected.

9.1.2 Wetting degradation indicators

FM	Contact angle	Drop stabilization time (seconds)
Sintono Terra HLK - Locolub (50%w/w)	59.8º	2.3
Tribolub - Locolub	47.5º	1.8

Table 9.1.2

Wetting results show a better perfomance for Tribolub, a lower contact angle and stabilization time required for the droplet to form on the rail surface. Although degraded samples could not be analyzed due to the lack of proper amounts of lubricant, this test show a more favorable contact angle and drop stabilization time for Tribolub than for Sintono Terra HLK, something that can be related to Sintono Terra higher viscosity a feature that causes a lower perfomance of its degraded counterpart when tested using the twin-disc machine.

9.1.3 Tribological indicators

The table 9.1 below resumes the following information; Friction coefficient, average wear, average wheel wear and average rail wear for degraded Sintono Terra HLK and Tribolub-3. Tribolub-3 perfomed better in the tribological test, a lower friction coefficient is observed besides a better average wear compared to Sintono Terra HLK.

Rheological behavior may be related with this performance, being Sintono Terra HLK a lubricant with an extremely high viscosity even more after suffering degradation, thus giving poor wetting results and for this reason a poor lubricating film onto the surface.

FM	Friction coefficient ($\bar{x}$)	Average wear (wheel-rail)	Average wear wheel	Average wear rail
Sintono Terra HLK	0.2273	0.103925	0.08765	0.1202
Tribolub-3	0.2137	0.09245	0.12145	0.0658

Table 9.1.3

10   Conclusions

Regarding the experimental methods

- It was shown that Brookfield viscometers could be considered as a low cost alternative for studying grease degradation using LV4 and 5 spindles when viscosity readings alone are required, even using a portable device, or SC4 spindles for obtaining precise shear stress and shear rate calculations.

- Particle analysis using an optical microscope gave an acceptable overview, compared with SEM results, for each lubricant and may be used as a simple approach to study particle distribution and morphology for degraded greases.

- Tribological testing of degraded greases using a twin-disc machine and a subsequent viscometric analysis can be considered as a viable option to study performance of degraded greases used for wheel-rail systems

Regarding the results of characterization of greases

- All the greases tested in this work showed a decrease in their tribological performance after mechanical degradation in twin-disc testing machine, being the degraded Tribolub-3 the one that

allowed obtaining lower values of friction coefficient and mass loss of the samples.

- Viscosity-time curves showed a rheopectic behavior at low shear rates for Sintono Terra HLK and Tribolub-3, which was related to the particle contents and the effect of thickeners.

- Metallic particles acted as catalyzers inducing a low temperature oxidation process as shown in the rheograms for photo degraded samples. Sintono Terra HLK proved to be more capable to withstand this degradation process, while Tribolub was severely degraded using this method.

- Wetting tests showed better wettability for Tribolub than for Sintono Terra HLK, both before and after degradation. This could result in a better performance in the lubrication system for the wheel-rail system.

- Both mechanical and radiation-induced degradation led to a significant increase in the viscosity of the greases studied, especially for low shear rates. FTIR analyses showed that such response was mainly caused by chemical changes in the structure of the greases.

11   BIBLIOGRAFY & REFERENCES

1. Mang T, Dresel W. Lubricants and Lubrication. Wiley; 2007. 906 p.

2. Bartels T, Bock W, Braun J, Busch C, Buss W, Dresel W, et al. Lubricants and Lubrication. Ullmann's Encyclopedia of Industrial Chemistry [Internet]. Wiley-VCH Verlag GmbH & Co. KGaA; 2000 [cited 2012 Nov 19]. Available from: http://onlinelibrary.wiley.com/doi/10.1002/14356007.a15_423/abstract

3. Hamrock BJ, Schmid SR, Jacobson BO. Fundamentals of Fluid Film Lubrication. Taylor & Francis; 2004. 736 p.

4. Bob Tuzik. Controlling Friction on Rail Transit Systems [Internet]. Interface - The Journal of Wheel/Rail Interaction. 2007 [cited 2013 Oct 8]. Available from: http://www.interfacejournal.com/features/01-07/friction_control/1.html

5. Santa JF. Development of a lubrication system for wear and friction control in wheel/rail interfaces. [Medellín]: Universidad Nacional de Colombia; 2007.

6. Barnes HA. A Handbook of elementary rheology. University of Wales, Institute of Non-Newtonian Fluid Mechanics; 2000. 224 p.

7. Mittal KL. Contact Angle, Wettability and Adhesion. BRILL; 2009. 412 p.

8. Loeb GI, Schrader ME. Modern Approaches to Wettability. Springer; 1992. 483 p.

9. Ali A, Lockwood F, Klaus EE, Duda JL, Tewksbury EJ. The Chemical Degradation of Ester Lubricants. A S L E Transactions. 1979;22(3):267–76.

10. Mortier RM, Fox MF, Orszulik ST. Chemistry and Technology of Lubricants. Springer; 2011. 561 p.

11. Gallardo-Hernandez EA, Lewis R, Dwyer-Joyce RS. Temperature in a twin-disc wheel/rail contact simulation. Tribology International. 2006 Dec;39(12):1653–63.

12. Rudnick LR. Lubricant Additives: Chemistry and Applications. Taylor & Francis; 2003. 766 p.

13. LUBRICANTES, BENLLOCH MARÍA, JOSÉ, ISBN: 9788432934148 [Internet]. [cited 2012 Nov 23]. Available from:

http://www.libreriaproteo.com/libro/ver/id/104226/titulo/lubricantes.html

14. Wilson LJ, Hargreaves DJ, Clegg RE, Powell J. Methodology for Measurement of Lubricant Decay Rate for Rail Lubricants [Internet]. 2008 [cited 2012 Nov 15]. Available from: http://eprints.qut.edu.au/13601/

15. Suzuki A, Ulfiati R, Masuko M. Evaluation of antioxidants in rapeseed oils for railway application. Tribology International. 2009 Jun;42(6):987–94.

16. Crutcher DE, Gervais R, Toms LA. Use of FT-IR Spectrometry as a Replacement for Physical Property Testing of Railway Lubricants. 1996 Apr.

17. Gorritxategi E. Nuevo método para la evaluación del estado de calidad del lubricante basado en análisis espectrométrico visible. Mantenimiento: ingeniería industrial y de edificios. 2008; (220):29–40.

18. Descartes S, Desrayaud C, Berthier Y. Experimental identification and characterization of the effects of contaminants in the wheel—rail contact. Proceedings of the Institution of Mechanical Engineers, Part F: Journal of Rail and Rapid Transit. 2008 Mar 1;222(2):207–16.